

Montana Tech Library

Digital Commons @ Montana Tech

---

Graduate Theses & Non-Theses

Student Scholarship

---

Spring 2020

**EFFECT OF FROTHER STRENGTH AND SOLIDS ON GAS  
DISPERSION IN A CAVITATION SPARGER MEASURED BY  
ELECTRICAL RESISTANCE TOMOGRAPHY**

Philip Holdsworth

Follow this and additional works at: [https://digitalcommons.mtech.edu/grad\\_rsched](https://digitalcommons.mtech.edu/grad_rsched)



Part of the [Metallurgy Commons](#)

---

EFFECT OF FROTHER STRENGTH AND SOLIDS ON GAS DISPERSION  
IN A CAVITATION SPARGER MEASURED BY ELECTRICAL  
RESISTANCE TOMOGRAPHY

By

Philip C. Holdsworth

A thesis submitted in partial fulfillment of the  
requirements for the degree of

Master of Science in Metallurgical/Mineral Processing Engineering

Montana Tech

2020



## Abstract

Gas dispersion in column flotation is critical for optimizing particle-bubble interaction and maximizing recovery. The effect of various flotation frothers on axial gas dispersion rates in a column flotation cell were measured using electrical resistance tomography (ERT). Tests included two-phase (gas-liquid) and three-phase (gas-liquid-solid) to determine the effect of mechanical parameters and the presence of solids on gas dispersion. Gas holdup can be measured using ERT and utilized in the determination of axial gas dispersion rate in the column. The ERT is constructed with two sensor planes making it possible to simultaneously capture gas holdup values at one cm and seven cm above the cavitation sparger. Three frothers of varying strengths were used to investigate axial dispersion rates. Experimental conditions were modified by altering the superficial gas rate, frother concentration, and sparger pump speed. The effects of varying experimental conditions were captured and are represented using concentration tomograms. There is a strong positive correlation between axial dispersion rate, frother strength, and machine operating parameters.

## **Dedication**

I dedicate this to my wife, Amy, and my children. They have offered continual support, encouragement and input throughout the process.

## **Acknowledgements**

The author thanks his family for their encouragement and patience during this process. He acknowledges Dr. Courtney Young for providing the opportunity to work on this project. The author thanks Dr. Richard LaDouceur for his extensive help in the preparation and analysis of the experiments and data involved in making this project a success. The author thanks the faculty of the Metallurgical Engineering program at Montana Tech for providing demanding and rewarding course work that provided the solid foundation needed to understand and carry out the work necessary to complete the course of study.

The author acknowledges the excellent facilities provided by Montana Tech that allowed this work to be carried out. Army Research Laboratories provided funding for this project and the author gratefully acknowledges their contribution.

## Table of Contents

<b>ABSTRACT .....</b>	<b>II</b>
<b>DEDICATION .....</b>	<b>III</b>
<b>ACKNOWLEDGEMENTS .....</b>	<b>IV</b>
<b>LIST OF TABLES.....</b>	<b>VI</b>
<b>LIST OF FIGURES.....</b>	<b>VII</b>
<b>LIST OF EQUATIONS .....</b>	<b>IX</b>
1. INTRODUCTION .....	1
2. METHODOLOGY .....	6
2.1. <i>Experimental set-up</i> .....	6
2.2. <i>ERT set-up</i> .....	7
2.3. <i>Two-phase test procedures</i> .....	10
2.4. <i>Three-phase test procedures</i> .....	11
2.4.1. Three-phase material preparation .....	12
3. TWO-PHASE RESULTS.....	15
3.1. <i>Two-phase gas holdup comparisons</i> .....	15
3.2 GAS HOLDUP RATE .....	26
4. 3.2 GAS HOLDUP RATE .....	26
5. THREE-PHASE RESULTS .....	31
5.1. <i>Three-phase results and comparisons</i> .....	31
5.1.1. MIBC Results .....	32
5.1.2. H27C Results .....	34
5.1.3. W31 Results .....	36
5.1.4. H27C block test results.....	38
5.2. <i>Three-phase results discussion</i> .....	41
6. CONCLUSIONS AND FUTURE WORK .....	42
<b>REFERENCES.....</b>	<b>43</b>

## List of Tables

Table I: Design of Experiment Factors .....	10
Table II: Talc ball mill feed and ball mill product distribution .....	13
Table III: MIBC gas holdup results for two-phase tests .....	15
Table IV: H27C gas holdup results for two-phase tests .....	15
Table V: W31 gas holdup results for two-phase tests.....	16
Table VI: ANOVA for all Experimental Results.....	17
Table VII: Statistical measures for frothers at Plane 1 and Plane 2.....	18
Table VIII: Gas Holdup Comparison 5 PPM.....	19
Table IX: Gas Holdup comparison 25 PPM .....	20
Table X: Change in gas holdup relative to air flow change.....	21
Table XI: Change in gas holdup rate relative to RPM change .....	21
Table XII: Plane 2 to Plane 3 Gas Holdup 5 ppm.....	25
Table XIII: Plane 2 to Plane 3 Gas Holdup 25 PPM .....	25
Table XIV: Gas holdup increase percentage .....	26
Table XV: Gas dispersion rates .....	27
Table XVI: Plane 2 to Plane 3 mean gas dispersion rate comparison .....	30
Table XVII: Three-phase ANOVA results .....	31
Table XVIII: MIBC Three-phase test results.....	32
Table XIX: H27C three-phase test results .....	35
Table XX: W31 three-phase test results .....	37
Table XXI: Block test ANOVA results .....	39
Table XXII: Block test confirmation results.....	39

## List of Figures

Figure 1: Eriez CavTube sparger .....	4
Figure 2: Flotation column layout showing pump, inputs, ERT sensor planes and tails outlet.....	7
Figure 3: Concentration tomogram showing plane 1 (P1) and plane 2 (P2) gas holdup concentrations .....	9
Figure 4: Decrease in gas holdup showing effect of frother adsorption .....	12
Figure 5: Ball mill feed and product size distribution .....	14
Figure 6: $\varepsilon_g$ comparisons of all frothers types at 5 ppm concentration.....	19
Figure 7: $\varepsilon_g$ comparisons of all frothers types at 25 ppm concentration.....	20
Figure 8: MIBC, Plane 1, 5 ppm.....	22
Figure 9: MIBC, Plane 2, 5 ppm.....	22
Figure 10: MIBC, Plane 1, 25 ppm.....	22
Figure 11: MIBC, Plane 2, 25 ppm.....	22
Figure 12: H27C, Plane 1, 5 ppm .....	23
Figure 13: H27C, Plane 2, 5 ppm .....	23
Figure 14: H27C, Plane 1, 25 ppm .....	23
Figure 15: H27C, Plane 2, 25 ppm .....	23
Figure 16: W31, Plane 1, 5 ppm .....	24
Figure 17: W31, Plane 2, 5 ppm .....	24
Figure 18: W31, Plane 1, 25 ppm .....	24
Figure 19: W31, Plane 2, 25 ppm .....	24
Figure 20: $E_g$ , MIBC .....	28
Figure 21: $E_g$ , H27C .....	28



Figure 22: $E_g$ , W31 .....	29
Figure 23: MIBC plane 1 gas holdup results .....	34
Figure 24: MIBC plane 2 gas holdup results .....	34
Figure 25: MIBC mean gas holdup results .....	34
Figure 26: MIBC $E_g$ results.....	34
Figure 27: H27C plane 1 gas holdup results.....	36
Figure 28: H27C plane 2 gas holdup results.....	36
Figure 29: H27C mean gas holdup results.....	36
Figure 30: H27C $E_g$ results .....	36
Figure 31: W31 plane 1 gas holdup results.....	38
Figure 32: W31 plane 2 gas holdup results.....	38
Figure 33: W31 mean gas holdup results.....	38
Figure 34: W31 $E_g$ results .....	38
Figure 35: Plane 1 gas holdup for H27C block test.....	40
Figure 36: Plane 2 gas holdup for H27C block test.....	40
Figure 37: Mean gas holdup for H27C block test.....	40
Figure 38: $E_g$ for H27C block test.....	40

## List of Equations

Equation (1) .....	8
Equation (2) .....	<b>Error! Bookmark not defined.</b>
Equation (3) .....	26

## 1. Introduction

Flotation is a fundamental method of solid-solid separation used for the recovery of valuable minerals from ore (Wills, et al., 2016). Flotation uses air introduced into a liquid or ore slurry through aspiration or a pressurized air system to create bubbles. The air is sheared through an impeller, diffuser, or cavitation device, creating a swarm of bubbles which rise through the liquid to the surface of the flotation cell. Gas holdup ( $\epsilon_g$ ) in flotation is a measure of the volume of air present in the flotation cell in the form of bubbles (Finch, et al., 1990). To establish the effects of frother strength on  $\epsilon_g$ , experiments were designed for a two-phase system. These tests demonstrated the differences between three frothers and their effect on  $\epsilon_g$ .

After establishing the effects on  $\epsilon_g$  with two-phase tests, three-phase tests were designed using talc, a naturally hydrophobic mineral. The ability of the valuable constituents in the ore to attach to bubble surfaces and be transported out of the liquid phase is dependent on the hydrophobicity of the particles. Most valuable mineral constituents in ore are not naturally hydrophobic which necessitates the addition of a collector. Collectors change the surface chemistry of the ore, inducing hydrophobicity, making different ore species amenable to flotation (Wills, et al., 2016). The use of talc eliminates the need to add a collector, making it unnecessary to quantify the effect of an additional variable (solution chemistry) and its effect on  $\epsilon_g$  (Banisi, 1995).

Gas dispersion in flotation is critical in maximizing particle-bubble collision rates in the collection zone of a flotation column (Zhou et al, 1994). Liquid and solid axial dispersion in flotation has been modeled and is well defined for bubble columns (Dobby and Finch, 1984). Conversely, published data on the axial dispersion rate of the bubble swarm generated in flotation is scarce. Using a hydrodynamic cavitation sparger for bubble generation, electrical

resistance tomography (ERT) was used to determine gas holdup values and the axial dispersion rate of the bubble swarm. Multiple frothers were tested to compare performance in the column. Frothers enhance the control of bubble size in the column and promote bubble stability, improving gas dispersion and gas holdup (Kuan and Finch, 2010). Parameters controlled were air flow rate, sparger pump speed and frother concentration.

Solution chemistry influences flotation results and any discussion of bubble formation, size and stability must recognize chemistry and machine interaction (Nesset, 2005). Frothers are added to the slurry to promote bubble formation and stabilize the bubbles by preventing coalescence. Azgomi et al. (2006) tested a variety of frothers, comparing chemistry and classifying differences using gas holdup. It has been shown that frother concentration has a marked effect on bubble size which is strongly correlated to gas holdup. (Cho and Laskowski, 2001, Azgomi et al, 2007, Banisi and Finch, 1994). The concentration of frother affects gas holdup and the axial dispersion rate. Bubble stability is dependent on the mechanical strength imparted to the bubble by the surfactants used in flotation (Zhou et al., 1994). Cho and Laskowski classified frothers by their ability to decrease bubble size and increase bubble stability (strength). Froth stability is also affected by particle size as shown by Farrokhpay and Bradshaw in their review of research on clay minerals in froth flotation (Farrakhpay, et al., 2012). Frothers were chosen to test the effect of strength and performance characteristics on gas holdup. Critical coalescence concentration (CCC) is a measure of the frother concentration at which bubble coalescence is prevented (Cho and Laskowski, 2002). Concentrations were selected that were below, near and above the CCC.

Gas dispersion in flotation is quantified by superficial gas velocity (volumetric air flow rate per cross-sectional area,  $J_g$ ), gas holdup (volumetric fraction of gas in liquid or liquid-slurry,

$\epsilon_g$ ) and bubble size distribution ( $D_b$ ) (Gomez and Finch, 2007). The use of  $J_g$  allows gas dispersion comparisons to be made between columns with varying cross-sectional areas. Hydrodynamic cavitation was used for bubble generation because of the ability to produce nano-bubbles (NB) and micro-bubbles (MB) (Ross et al., 2019). Zhou et al. (2009) discuss the effect of liquid velocity on gas holdup when using a cavitation tube for bubble generation. As shown in Figure 1, the design of the column has the pump feeding directly to the cavitation device. The pump speed controls fluid velocity and by association the amount of pressure drop through the cavitation tube which is critical to bubble formation and gas holdup. By creating a pressure drop, fluid pressure is lowered below the vapor pressure, resulting in the creation of NB and MB at the outlet of the sparger. Eriez, a manufacturer of flotation equipment, supplied a Cavtube sparger, shown in **Figure 1**, a type of hydrodynamic cavitation device (HCD), for bubble generation in the column.

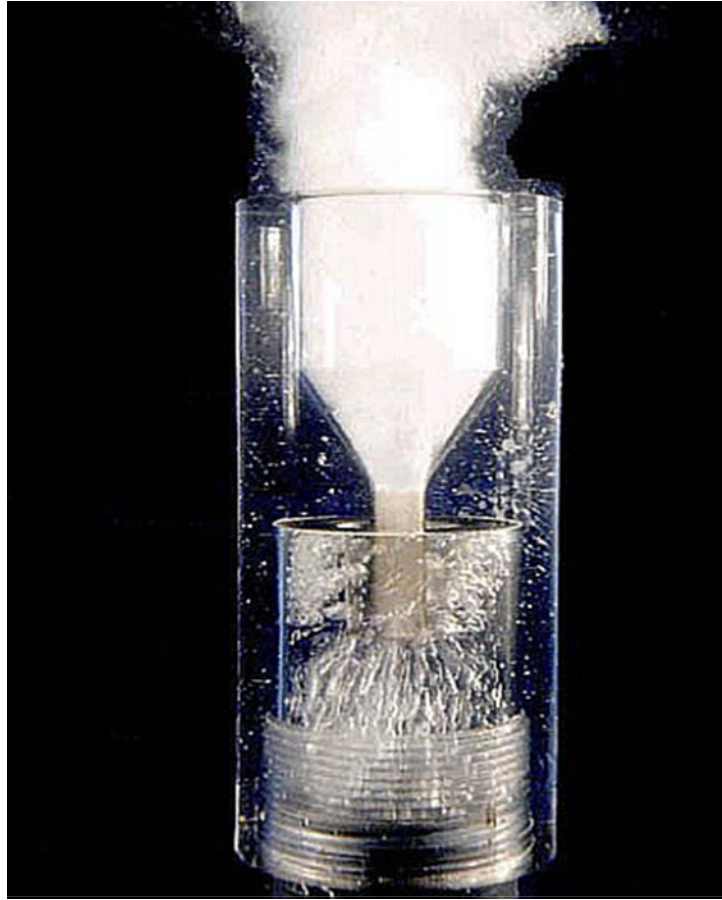


**Figure 1: Eriez CavTube sparger**

Combined with the shearing of additional gas, added between the pump and sparger, cavitation creates a supply of bubbles suitable for a range of particle sizes (Zhou, et al., 2009). Control of the additional air volume has a pronounced effect on the gas holdup in the column. Numerous sensors and devices have been used to measure gas dispersion in flotation machines and have been described elsewhere (Azgomi, et al., 2007). ERT uses conductivity changes in a fluid to measure gas holdup. Air bubbles in the liquid are highly conductive on the surface while the gas in the bubble has very low conductance. This effect can be measured by electrodes installed on the boundary of the column. Electrodes are arranged around the perimeter of a pipe and a current is applied to the fluid through the electrodes. The voltages on the electrodes are

measured and the conductivity of the fluid for the cross section of the column is reconstructed using the measured voltages and known currents (Nissinen et al., 2014). The conductivity is displayed as a concentration tomogram, showing radial profiles of gas holdup in the flotation column. The accuracy of gas holdup measurements using the ERT have been compared to pressure transducers by Vadlakonda et al. (2018) and found to have minimum and maximum errors of 0.57% and 4.47% respectively. Singh et al. (2013) performed tests in a bubble column comparing ERT to voidage probe measurements and found that gas holdup values were closely aligned except at very low values (<2%) and very high values (>30%).

## 2. Methodology

### 2.1. Experimental set-up

**Figure 2** shows a schematic of the flotation column and installation locations of the ERT sensor. The location of the ERT sensor immediately above the sparger enables the capture of two distinct gas holdup measurements as the bubbles exit the sparger and enter the column. Plane 1 and plane 2 measurements were taken from this location. Plane 3 and plane 4 measurements were taken from the middle location shown in the schematic. The measurements from planes 3 and 4 were used to compare the gas holdup in the quiescent zone to the collection zone, immediately above the sparger. Gas holdup was tested using two phase (gas-water) and three phase (gas-water-solid) mixtures with the conductivity of the water and slurry adjusted to  $\sim 10\text{mS}$  for resolution. Frothers tested were methyl isobutyl carbinol (MIBC), polyoxyalkylene alkyl ether (H27C), and polypropylene glycol methyl ether (W31), the latter two supplied by Huntsman Chemical. H27C produces a moderately stronger froth than MIBC but is soluble in water. W31 is comparable to DowFroth 250, produces an intermediate strength froth and provides an increase in froth stability over the other frothers. Dried, pressurized air at 550 KPa (5.5 bar) is introduced at the bottom of the sparger as shown in **Figure 2**. Air is routed through a pressure regulator and rotameter to control total volume delivered to the sparger. A centrifugal pump is used to pressurize the fluid passing through the sparger and is powered by a 373 W (1/2 HP) motor with a DC drive, allowing variable pump speeds from 0-3100 RPM.



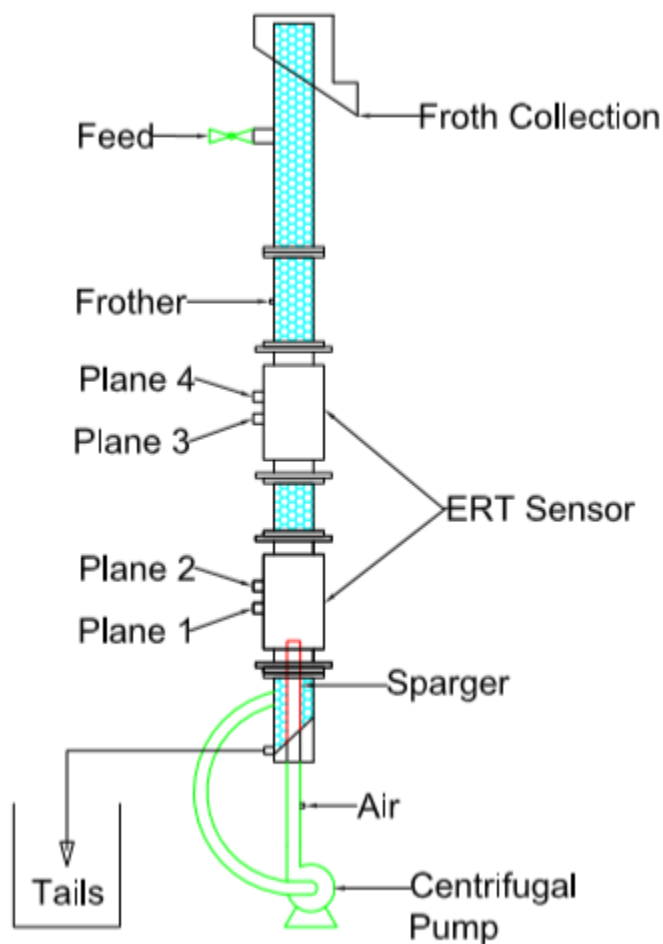


**Figure 2: Flotation column layout showing pump, inputs, ERT sensor planes and tails outlet.**

## 2.2. ERT set-up

The ERT equipment has three parts: sensor, data acquisition system (DAS) and personal computer. Industrial Tomography Systems (ITS) supplied a 32-electrode pipe sensor with the sensors divided into 2, 16 electrode planes. Electrodes are 2 cm x 1 cm and the planes are

separated by 5 cm, enabling separate data streams to be collected for each plane. Aw et al. (2013) discuss the importance of electrode placement and sizing to produce accurate results.

Signal processing and data collection are handled through the ITS p2+ instrument and software (DAS). ITS uses a simplified version of Maxwell's equation to calculate the non-conductive phase as shown in Equation 1. The non-conductive phase represents the air inside the bubbles and is used to calculate the total gas holdup. The conductive phase is calculated using the full Maxwell equation as shown in Equation **Error! Reference source not found.**. All calculations are completed by the software and gas holdup values are generated for each data frame.

$$\alpha = \frac{2\sigma_1 - 2\sigma_{mc}}{\sigma_{mc} - 2\sigma_1} \quad (1)$$

$$\alpha = \frac{2\sigma_1 + \sigma_2 - 2\sigma_{mc} - \frac{\sigma_{mc}\sigma_2}{\sigma_1}}{\sigma_{mc} - \frac{\sigma_2}{\sigma_1}\sigma_{mc} + 2(\sigma_1 - \sigma_2)} \quad (2)$$

$\alpha$  = volume fraction of dispersed phase

$\sigma_1$  = conductivity of dispersed phase

$\sigma_2$  = conductivity of continuous phase

$\sigma_{mc}$  = reconstructed measured conductivity

A desktop computer is used to interface with the system and allows real-time gas holdup visualization and export of the tomographic data. Gas holdup is displayed as a concentration tomogram, **Figure 3**, using a color scale display showing variations in concentration over the

cross section of the column. In **Figure 3**, red represents the highest concentration of gas while blue is the lowest concentration. The color gradation from blue to red represents increasing gas holdup. Data is exported in .csv format to Microsoft Excel, allowing initial formatting prior to analysis in Design Expert statistical software.

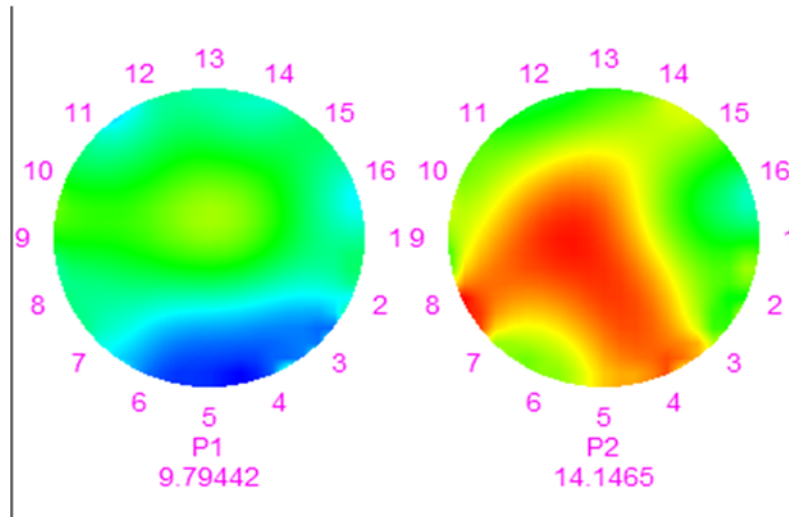


**Figure 3: Concentration tomogram showing plane 1 (P1) and plane 2 (P2) gas holdup concentrations**

Before collecting data, it is necessary to fill the column and calibrate the conductivity and gain of the liquid or slurry and take reference measurements relative to a known reference. This procedure must be repeated for each change in experimental parameters. Fluid conductivity is measured and adjusted for each new test. The column is emptied and cleaned between concentration tests of the same frother and when frother types are changed in order to ensure consistent results.

Measurement of the axial dispersion in the column was accomplished by aligning the ERT sensor to capture gas dispersion effects as the bubble swarm developed near the outlet of the sparger. To allow comparison of the gas holdup between the area near the sparger and higher

in the column, experiments were repeated with the ERT sensor placed in the quiescent zone. This area is shown as plane 3 and plane 4 in **Figure 2**.

### 2.3. Two-phase test procedures

Upper and lower limits for the three most influential factors were determined through testing and were found to give stable operation within the column. Factors that had the highest response were pump speed, air volume and frother concentration. Pump speed effects sparger performance in bubble production, air volume effects total gas holdup and frother concentration controls bubble stability and formation. Using Design Expert software from Stat-Ease, a two-level factorial experiment (with midpoints to test for curvature) was created, consisting of 11 tests. Each frother was tested using the conditions in the design of experiment. **Error! Reference source not found.** shows the values used to create the upper and lower bounds for the design of experiment.

**Table I: Design of Experiment Factors**

Factor	Units	Low	High
Pump Speed	RPM	1500	2600
Air Volume	LPM	2.5	4.5
Concentration	PPM	5	25

The ITS system for ERT collects data in frames, each frame an average of electrode voltage measurements taken at approximately one second intervals. 150 frames were collected for each test, giving 1650 frames for each experiment. Each test was conducted with Butte, Montana tap water adjusted to a conductivity value of ~10mS using table salt (NaCl). A Mettler Toledo Seven Excellence Multiparameter meter with an Inlab 731 ISM probe was used for all

conductivity measurements. Vadlakonda (2018) showed that changes in liquid height affect gas holdup values so the liquid height was held constant for all tests. A pressure transducer coupled to the PLC was used to ensure consistent liquid height between experiments. Frother dosage was calculated as a function of column volume, with frother added from a dilute solution (2% by weight) by a peristaltic pump. Water was added at the same time to ensure complete mixing. The pump curve for the frother dosage pump was found through testing and linear regression was used to determine correct pump speed and timing for dosage requirements. The DC drive provides variable speed control of the pump motor and the installation of a digital tachometer allowed the pump RPM to be adjusted accurately. After starting the pump and air flow, data collection began after allowing time for bubbles to fill the full height of the column.

#### **2.4. Three-phase test procedures**

The goal of three-phase testing was to determine the interaction of frother concentration and solids content. The initial design of experiment frother concentration range was set from 5 to 25 ppm and solids concentration was set from 10 to 20 percent solids by weight. Due to the complexity of three-phase flow, air flow was fixed at 3.5 liters per minute, which equates to a superficial gas velocity ( $J_g$ ) of 1.13 cm/s, and pump speed was fixed at 2400 RPM. This made the statistical model simpler for the initial experiments. MIBC, H27C and W31 were all tested using the same parameters. Conductivity testing indicated that 85 grams of NaCl gave consistent results between 10.8 and 11.0 mS for each test.

As shown in **Figure 4** gas holdup decreases as the test progresses. This effect has also been shown to take place in the flotation of minerals with clay content (Farrakhpay, et al., 2012).

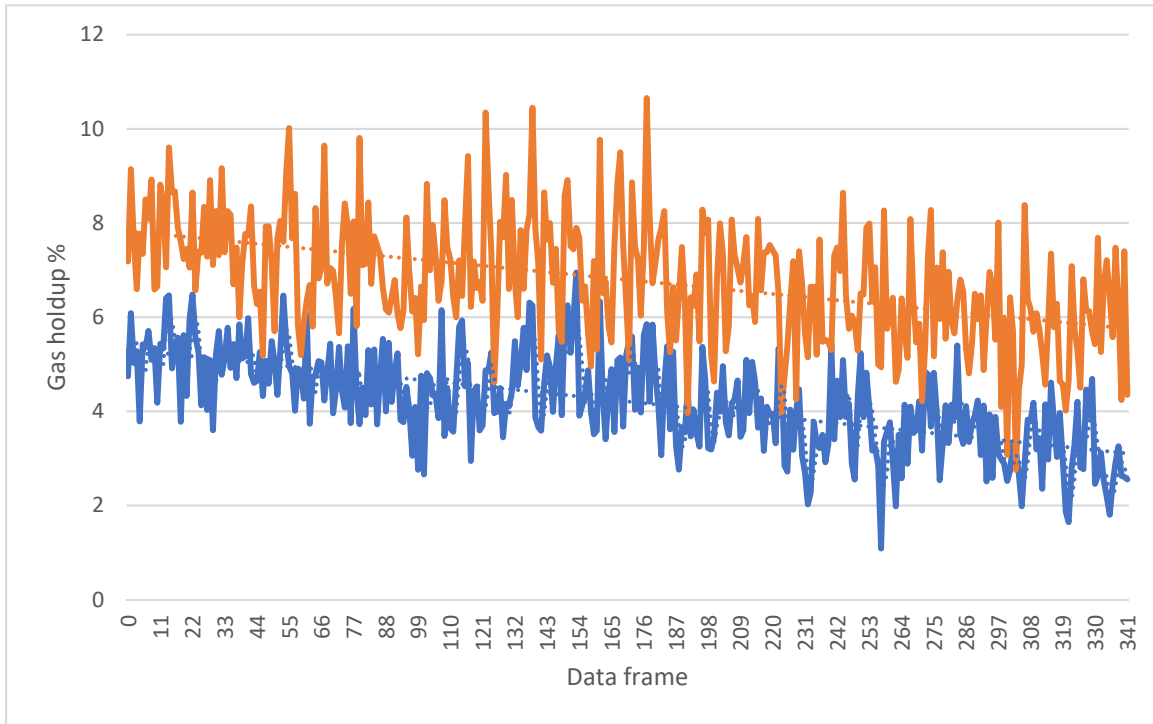


**Figure 4: Decrease in gas holdup showing effect of frother adsorption**

To limit the effects of frother adsorption on test results, frother was only added after complete mixing of the talc slurry and testing of the conductivity. Frother mixing time was limited to 60 seconds prior to filling the column and calibrating the ERT for each test. This reduced total time before beginning each test to less than five minutes, minimizing the effects of frother adsorption on gas holdup results.

#### **2.4.1. Three-phase material preparation**

Talc was selected for use in three-phase testing due to its naturally hydrophobic properties (Kuan, et al., 2010). Solution chemistry plays a role in flotation kinetics so eliminating the presence of a collector eliminates an additional variable that makes frother comparison more difficult (Nesset, 2005). Minerals Technologies in Dillon, Montana supplied raw talc ore for the three phase experiments. The raw talc was blended and reduced in a roll crusher to 5mm maximum particle size and a lab-scale ball mill was used to grind to the final product size.

Residence time in the ball mill was 30 minutes followed by screening of the 75 to 150  $\mu\text{m}$  size range. Oversize material was returned to the ball mill for additional grinding. The -150  $\mu\text{m}$  product was kept for future testing that will determine the effect of particle size on gas holdup. A Ro-Tap machine was used for all particle classifications. Particle distributions for the ball mill feed and product are shown in **Table II**.

**Table II: Talc ball mill feed and ball mill product distribution**

**Ball Mill Feed**

Screen	Retained	% Retained	Cum Mass Retained	Cum % Retained	% Passing
3/8	0	0.00%	0.00	0.00%	100.00%
20	272.8	65.48%	272.80	65.48%	34.52%
50	64.6	15.51%	337.40	80.99%	19.01%
70	15.2	3.65%	352.60	84.64%	15.36%
100	13.7	3.29%	366.30	87.93%	12.07%
200	18.2	4.37%	384.50	92.29%	7.71%
Pan	32.1	7.71%	416.60	100.00%	0.00%
Total Mass	416.6				

**Ball Mill Product**

Screen	Mass	% Retained	Cum Mass Retained	Cum % Retained	% Passing
3/8	0	0.00%	0.00	0.00%	100.00%
20	19.3	2.70%	19.30	2.70%	97.30%
50	10.3	1.44%	29.60	4.14%	95.86%
70	24.2	3.39%	53.80	7.53%	92.47%
100	138	19.31%	191.80	26.84%	73.16%
200	352	49.25%	543.80	76.09%	23.91%
Pan	170.9	23.91%	714.70	100.00%	0.00%
Total Mass	714.7				

**Figure 5** shows the product distribution curves for the ball mill feed and product. The  $P_{80}$  is near the 150  $\mu\text{m}$  top size for the flotation tests. Particle size used in the flotation experiments was 75 to 150  $\mu\text{m}$ . As particle size increases, coalescence efficiency decreases so the top size of

150  $\mu\text{m}$  was chosen to maintain the coalescence performance of the frothers chosen (Sarhan, et al., 2017).

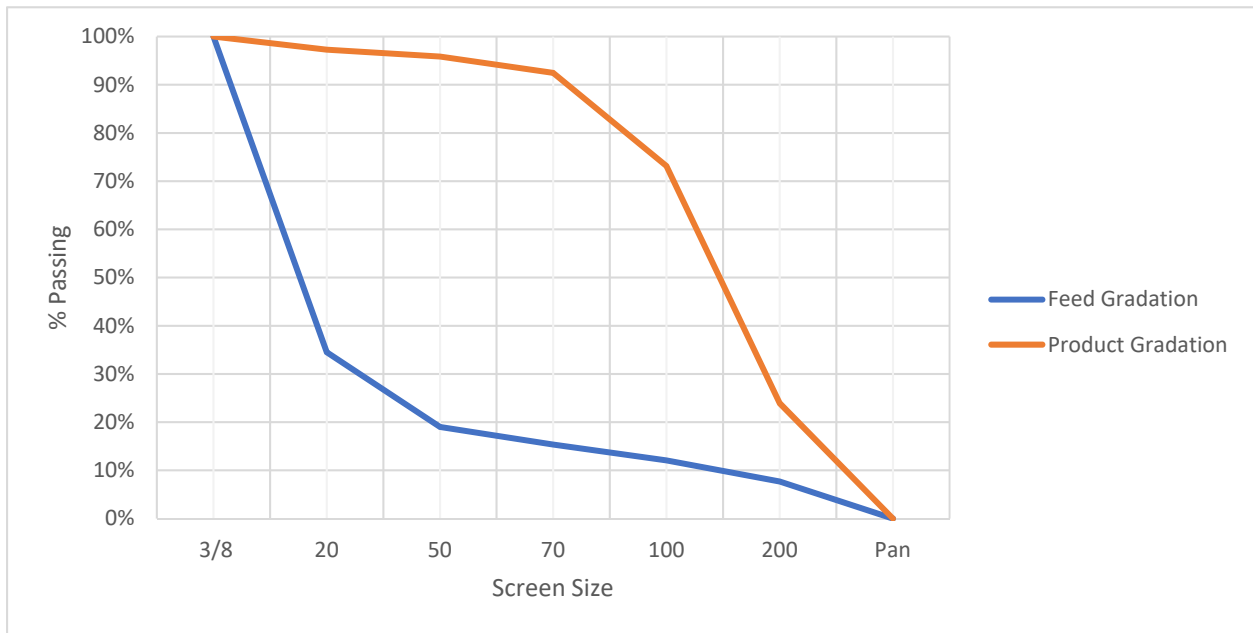


**Figure 5: Ball mill feed and product size distribution**



### 3. Two-phase Results

#### 3.1. Two-phase gas holdup comparisons

Raw data from the ITS DAS was scrubbed using Microsoft Excel and compiled by frother type prior to being exported to Design Expert for analysis. The results of all the two-phase tests for each frother are shown in **Table III**, **Table IV** and **Table V**. Values for Mean (the average of Plane 1 and Plane 2), Plane 1 and Plane 2 are all shown in percent gas holdup. The gas holdup values were exported to Design Expert and were analyzed for statistical significance.

**Table III: MIBC gas holdup results for two-phase tests**

Std	Run	A:Pump Speed	B:Air Volume	C:Concentration	Mean	Plane 1	Plane 2
10	1	2070	3.5	15	8.631	7.053	10.209
7	2	1540	4.5	25	7.646	6.019	9.273
6	3	2600	2.5	25	10.937	10.228	11.645
11	4	2070	3.5	15	9.459	8.022	10.897
2	5	2600	2.5	5	5.886	5.109	6.663
1	6	1540	2.5	5	4.490	3.473	5.506
4	7	2600	4.5	5	9.821	7.881	11.761
3	8	1540	4.5	5	6.208	4.722	7.694
8	9	2600	4.5	25	13.582	11.686	15.478
9	10	2070	3.5	15	9.555	8.063	11.047
5	11	1540	2.5	25	5.720	4.696	6.744

**Table IV: H27C gas holdup results for two-phase tests**

Std	Run	A:Pump Speed	B:Air Volume	C:Concentration	Mean	Plane 1	Plane 2
10	1	2070	3.5	15	10.495	9.058	11.932
7	2	1540	4.5	25	8.767	7.140	10.394
6	3	2600	2.5	25	12.456	11.966	12.946
11	4	2070	3.5	15	10.421	9.231	11.611
2	5	2600	2.5	5	9.686	9.027	10.346
1	6	1540	2.5	5	5.534	4.530	6.538
4	7	2600	4.5	5	12.412	10.753	14.070
3	8	1540	4.5	5	7.634	5.943	9.325
8	9	2600	4.5	25	14.399	12.730	16.068
9	10	2070	3.5	15	10.179	9.279	11.079
5	11	1540	2.5	25	5.663	4.582	6.754

**Table V: W31 gas holdup results for two-phase tests**

Std	Run	A:Pump Speed	B:Air Volume	C:Concentration	Mean	Plane 1	Plane 2
10	1	2070	3.5	15	11.631	10.459	12.803
7	2	1540	4.5	25	8.168	6.729	9.607
6	3	2600	2.5	25	12.475	11.917	13.034
11	4	2070	3.5	15	11.875	10.580	13.171
2	5	2600	2.5	5	11.099	10.649	11.549
1	6	1540	2.5	5	5.962	4.925	6.999
4	7	2600	4.5	5	13.766	11.854	15.678
3	8	1540	4.5	5	8.515	6.681	10.350
8	9	2600	4.5	25	15.672	13.931	17.413
9	10	2070	3.5	15	10.661	9.883	11.439
5	11	1540	2.5	25	6.950	5.808	8.092

Utilizing analysis of variance (ANOVA), Design Expert® tests the statistical validity of the results and creates an appropriate predictive model. Each test produced significant results and a model for each frother type was created. The ANOVA results for all tests are shown in **Table VI**. The p-values shown in the table are all less than 0.05, indicating that main effects A, B, C, and a two-factor interaction, AC, are all significant in each model. F-values indicate that results are not due to noise and that the lack of fit is not significant. A review of **Table VI** shows that all frother types produced significant results.

**Table VI: ANOVA for all Experimental Results**

		Model	A: Pump Speed	B: Air Volume	C: Concentration	Lack of fit	
MIBC	Mean	F-value	41.41	80.83	32.34	40.78	1.94
		p-value	0.0005	0.0003	0.0023	0.0014	0.3578
	Plane 1	F-value	51.79	111.8	20.21	57.23	0.7923
		p-value	0.0003	0.0001	0.0064	0.0006	0.5998
	Plane 2	F-value	19.86	27.13	18.95	13.49	8.73
		p-value	0.0016	0.002	0.0048	0.0104	0.1054
	E <sub>g</sub>	F-value	367.73	7.24	1051.11		0.9618
		p-value	0.0001	0.0361	0.0001		0.5671
H27C	Mean	F-value	189.73	575	122.88	45.67	5.38
		p-value	0.0001	0.0001	0.0001	0.0011	0.1608
	Plane 1	F-value	107.05	360.51	3032	27.6	20.52
		p-value	0.0001	0.0001	0.0027	0.0033	0.0468
	Plane 2	F-value	149.72	390.95	165.17	32.45	0.5287
		p-value	0.0001	0.0001	0.0001	0.0023	0.7059
	E <sub>g</sub>	F-value	143.64		143.64		0.2888
		p-value	0.0001		0.0001		0.9
W31	Mean	F-value	59.9	102.46	17.35		1.87
		p-value	0.0001	0.0001	0.0042		0.3841
	Plane 1	F-value	115.73	318.37	18.88	9.93	1.99
		p-value	0.0001	0.0001	0.0048	0.0198	0.3619
	Plane 2	F-value	44.43	65.85	23.01		1.23
		p-value	0.0001	0.0001	0.002		0.5042
	E <sub>g</sub>	F-value	81.46		81.46		0.8992
		p-value	0.0001		0.0001		0.8992

Additional statistical tests performed by Design Expert include coefficient of variance (CV), adequate precision,  $R^2$ , adjusted  $R^2$  and predicted R-squared. These values are shown in **Table VII** for all frothers tested.

**Table VII: Statistical measures for frothers at Plane 1 and Plane 2**

	MIBC		H27C		W31	
	Plane 1	Plane 2	Plane 1	Plane 2	Plane 1	Plane 2
<b>Std. Dev.</b>	0.535	1.110	0.415	0.365	0.480	0.986
<b>Mean</b>	7.000	9.720	8.567	11.006	9.400	11.830
<b>C.V. %</b>	7.640	11.400	4.843	3.318	5.100	8.330
<b>R<sup>2</sup></b>	0.976	0.909	0.988	0.992	0.983	0.927
<b>Adjusted R<sup>2</sup></b>	0.958	0.863	0.979	0.985	0.975	0.906
<b>Predicted R<sup>2</sup></b>	0.885	0.643	0.920	0.964	0.938	0.819
<b>Adeq Precision</b>	21.670	13.881	28.480	36.689	26.576	15.140

After completing the analysis of the individual frothers all tests were combined in Design Expert to create a general model. Gas holdup values gathered during testing fell in the 5-25% range, similar to results found in tests comparing ERT and pressure transducers (Singh, et al., 2017). Statistical analysis of data gathered in the tests performed in this study show that results are consistent and can be modeled reliably.

Using MS Excel, total gas holdup ( $\epsilon_g$ ) for each frother and test condition at 5 ppm and 25 ppm were tabulated and charted to compare results. **Table VIII** and **Table IX** are the compiled results of the  $\epsilon_g$  for each experiment. Figures 2a and 2b show direct comparisons of each plane for each test parameter.

Table VIII: Gas Holdup Comparison 5 PPM

PPM	RPM	1540	1540	2070	2600	2600
5	LPM	2.5	4.5	3.5	2.5	4.5
MIBC	Plane 1 $\epsilon_g$	3.47	4.72	7.71	5.11	7.88
	Plane 2 $\epsilon_g$	5.51	7.69	10.72	6.66	11.76
H27C	Plane 1 $\epsilon_g$	4.53	5.94	9.19	9.03	10.75
	Plane 2 $\epsilon_g$	6.54	9.32	11.54	10.35	14.07
W31	Plane 1 $\epsilon_g$	4.92	6.68	10.31	10.65	11.85
	Plane 2 $\epsilon_g$	7.00	10.35	12.47	11.55	15.68

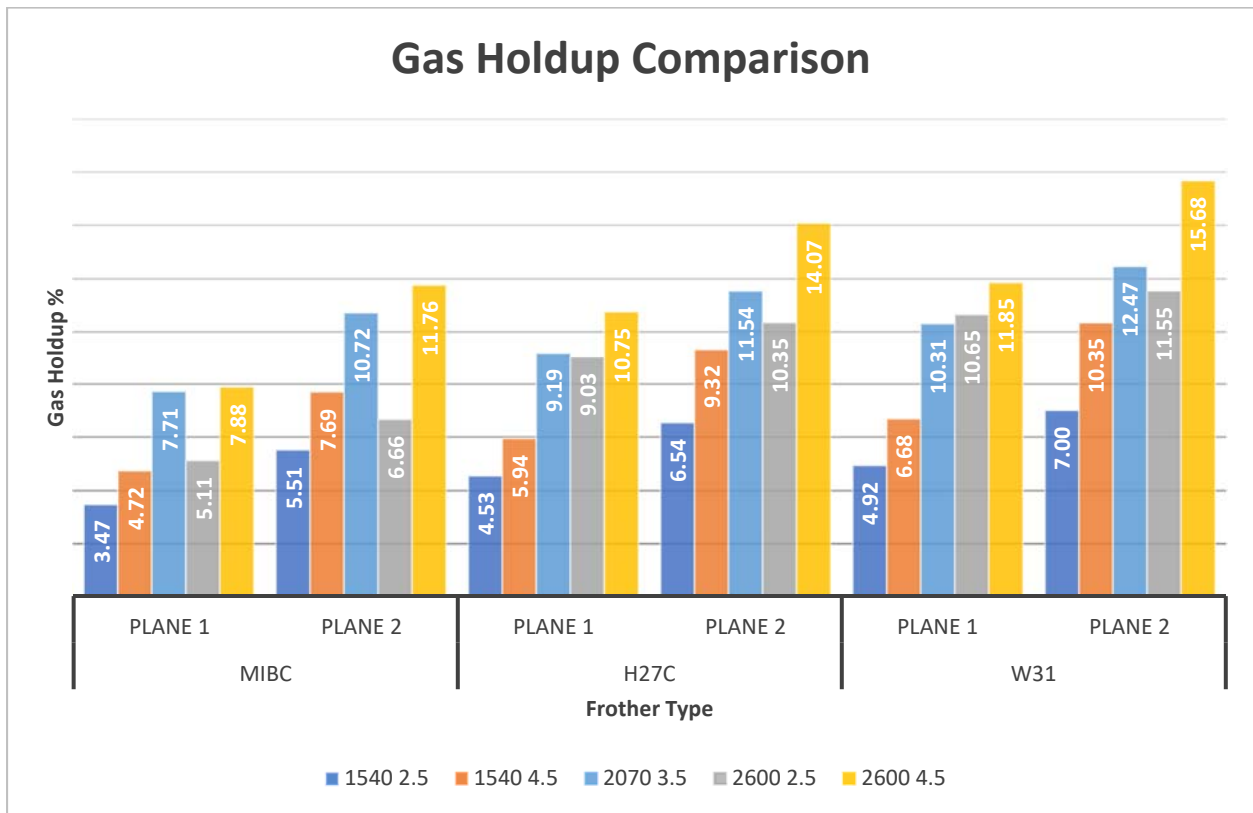
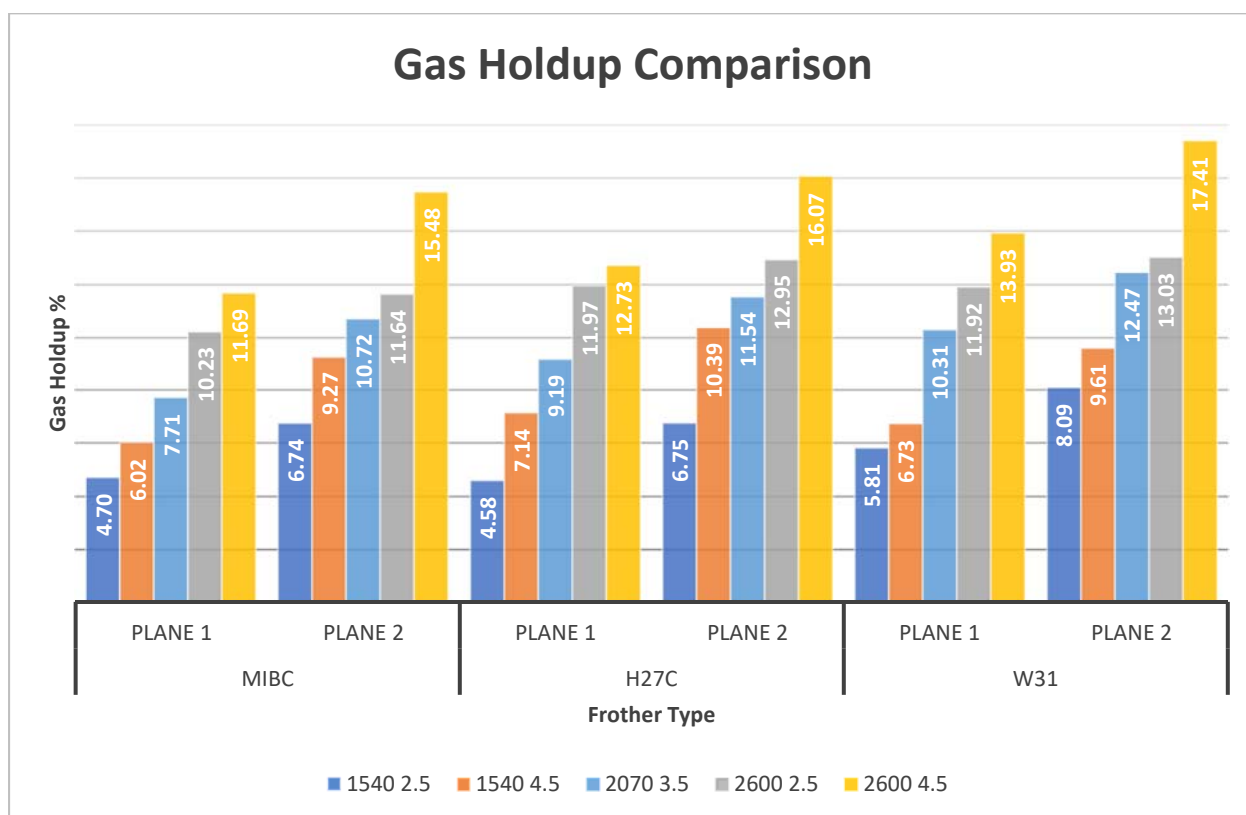
Figure 6:  $\epsilon_g$  comparisons of all frothers types at 5 ppm concentration

Table IX: Gas Holdup comparison 25 PPM

PPM	RPM	1540	1540	2070	2600	2600
25	LPM	2.5	4.5	3.5	2.5	4.5
MIBC	Plane 1 $\epsilon_g$	4.70	6.02	7.71	10.23	11.69
	Plane 2 $\epsilon_g$	6.74	9.27	10.72	11.64	15.48
H27C	Plane 1 $\epsilon_g$	4.58	7.14	9.19	11.97	12.73
	Plane 2 $\epsilon_g$	6.75	10.39	11.54	12.95	16.07
W31	Plane 1 $\epsilon_g$	5.81	6.73	10.31	11.92	13.93
	Plane 2 $\epsilon_g$	8.09	9.61	12.47	13.03	17.41

Figure 7:  $\epsilon_g$  comparisons of all frothers types at 25 ppm concentration

Using **Figure 6** and **Figure 7** as a starting point, charts were created in Design Expert to compare the influential factors simultaneously. **Figure 8** through **Figure 19** show 3-dimensional (3D) surfaces for the results of the 5 and 25 ppm tests comparing Plane 1 and Plane 2 of MIBC, H27C and W31, respectively. Pump speed and air flow are shown as x1-axis and x2-axis with gas holdup shown on the y-axis.

**Table X** quantifies the rate of change for gas holdup relative to changes in air flow. **Table XI** is similar but shows the rate as RPM increases.

**Table X: Change in gas holdup relative to air flow change**

	RPM	5 PPM			25 PPM		
		MIBC	H27C	W31	MIBC	H27C	W31
$d\varepsilon_g/dQ_{Air}$ Plane 1	1540	0.624	0.707	0.878	0.661	1.279	0.461
	2600	1.386	0.863	0.602	0.729	0.382	1.007
$d\varepsilon_g/dQ_{Air}$ Plane 2	1540	1.094	1.393	1.675	1.265	1.820	0.758
	2600	2.549	1.862	2.065	1.916	1.561	2.190

**Table XI: Change in gas holdup rate relative to RPM change**

	$Q_{air}$	5 PPM			25 PPM		
		MIBC	H27C	W31	MIBC	H27C	W31
$d\varepsilon_g/dV_{RPM}$ Plane 1	2.5	0.00154	0.00424	0.00540	0.00522	0.00697	0.00576
	4.5	0.00298	0.00454	0.00488	0.00535	0.00527	0.00679
$d\varepsilon_g/dV_{RPM}$ Plane 2	2.5	0.00109	0.00359	0.00429	0.00462	0.00584	0.00466
	4.5	0.00384	0.00448	0.00503	0.00585	0.00535	0.00736

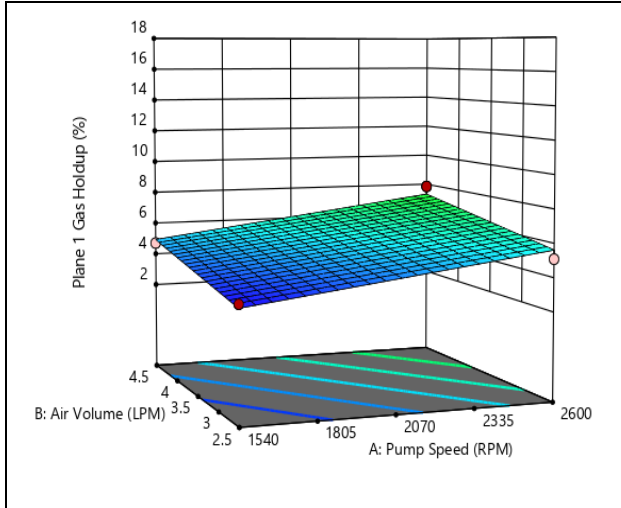


**Figure 8: MIBC, Plane 1, 5 ppm**

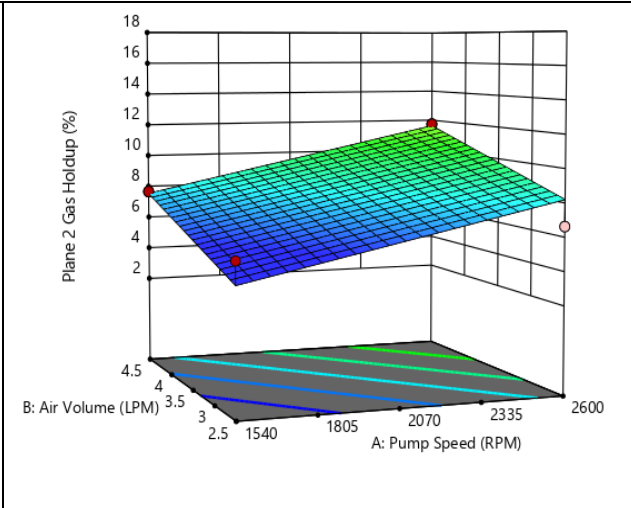


**Figure 9: MIBC, Plane 2, 5 ppm**

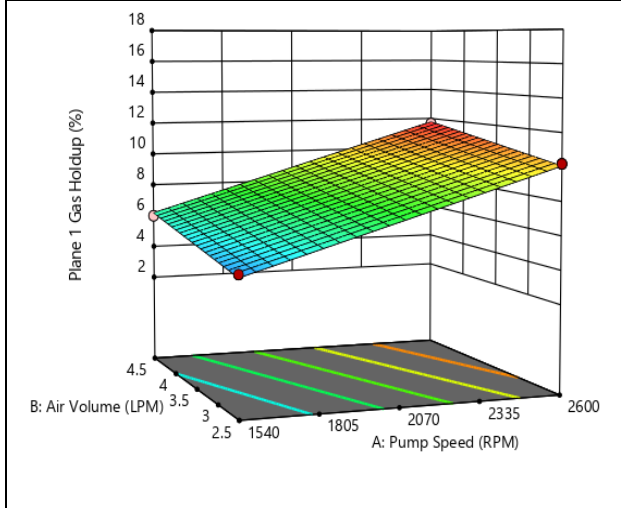


**Figure 10: MIBC, Plane 1, 25 ppm**

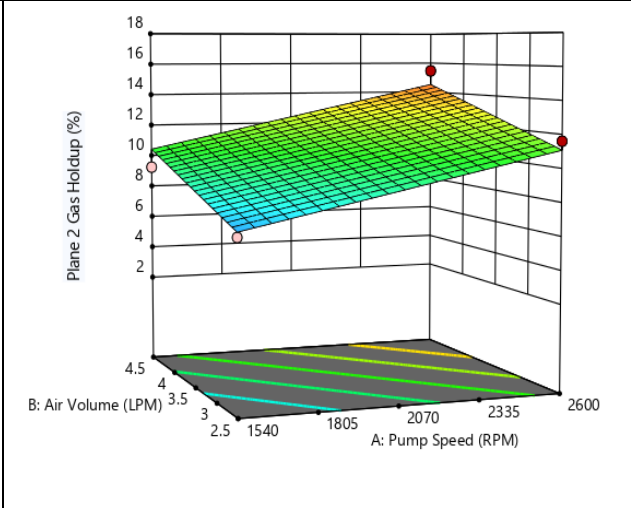


**Figure 11: MIBC, Plane 2, 25 ppm**



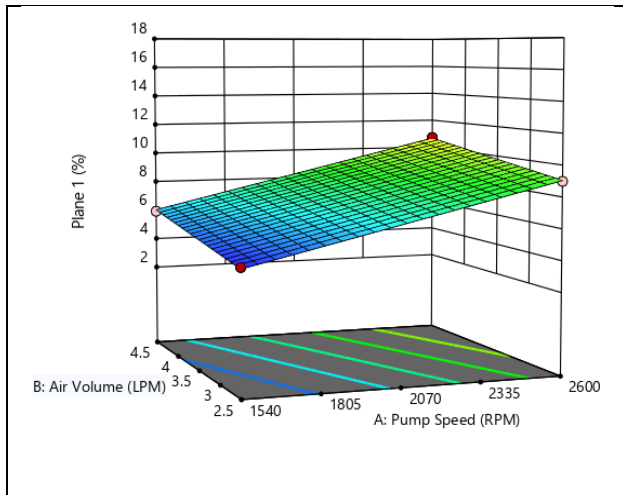


**Figure 12: H27C, Plane 1, 5 ppm**

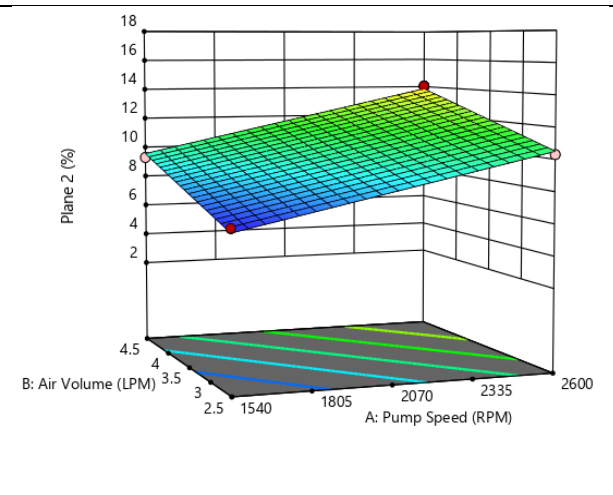


**Figure 13: H27C, Plane 2, 5 ppm**

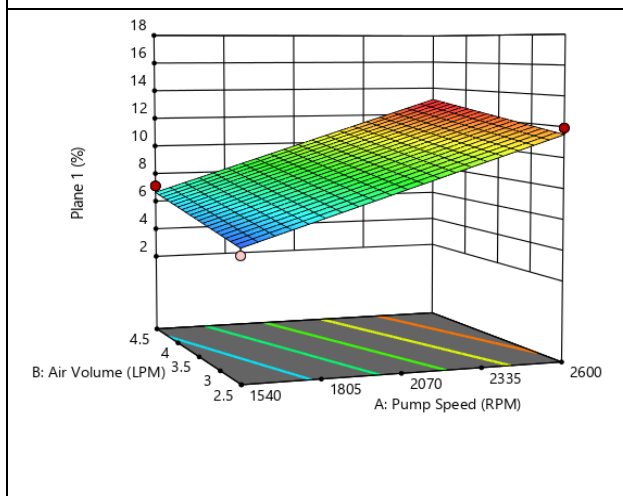


**Figure 14: H27C, Plane 1, 25 ppm**

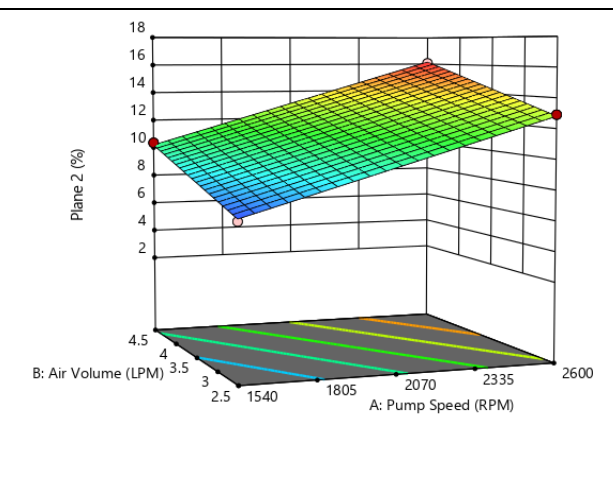


**Figure 15: H27C, Plane 2, 25 ppm**

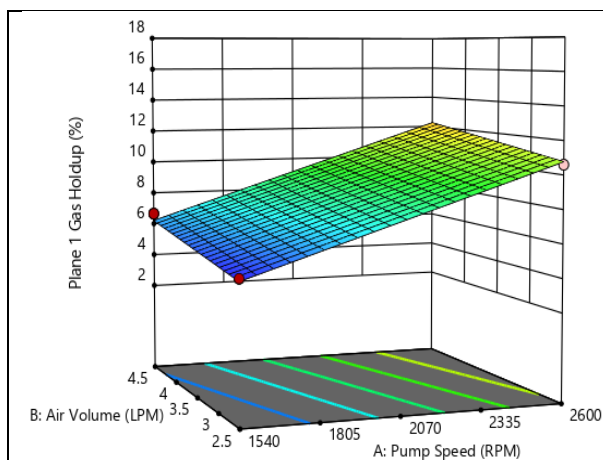


**Figure 16: W31, Plane 1, 5 ppm**

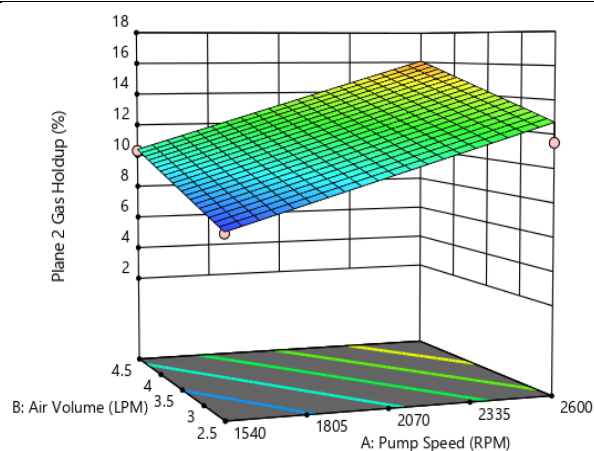


**Figure 17: W31, Plane 2, 5 ppm**

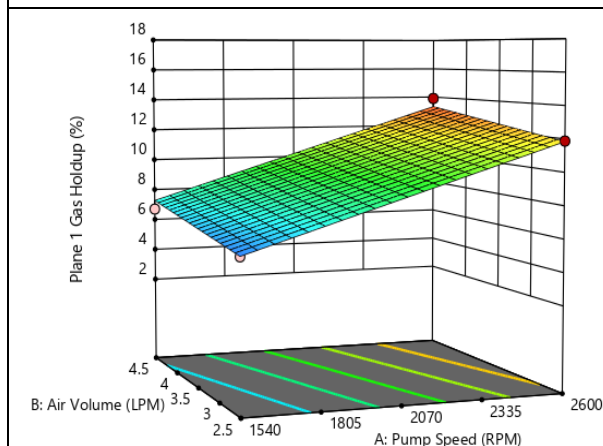


**Figure 18: W31, Plane 1, 25 ppm**

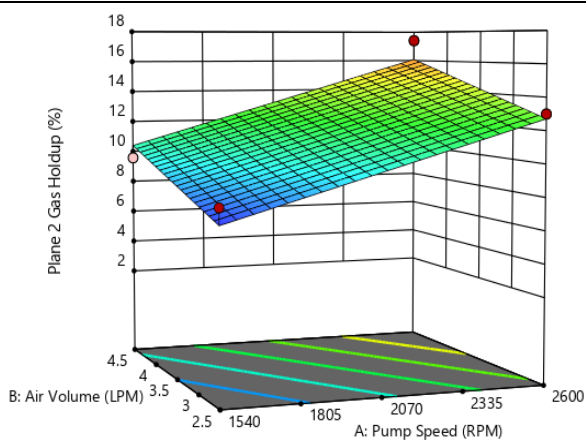


**Figure 19: W31, Plane 2, 25 ppm**

Comparisons of gas holdup results between plane 2 and plane 3 were made to determine if maximum gas holdup value is achieved near the sparger. **Table XII** and **Table XIII** show the results from the ERT and the differences in gas holdup values between plane 2 and plane 3. Values at 5 ppm show some instability relative to 25 ppm, having a maximum difference of -

4.53%, a loss from the maximum at the sparger. The 25 ppm tests have a maximum change of 1.98% over 40.5 cm, showing that gas holdup achieves maximum or near maximum values near the sparger.

**Table XII: Plane 2 to Plane 3 Gas Holdup 5 ppm**

PPM	RPM	1540	1540	2070	2600	2600
<b>5</b>	<b>LPM</b>	2.5	4.5	3.5	2.5	4.5
<b>MIBC</b>	<b>Plane 2 <math>\epsilon_g</math></b>	6.74	9.27	10.72	11.64	15.48
	<b>Plane 3 <math>\epsilon_g</math></b>	6.01	8.97	9.82	7.11	12.20
	<b><math>\Delta \epsilon_g</math></b>	-0.74	-0.30	-0.90	-4.53	-3.28
<b>H27C</b>	<b>Plane 2 <math>\epsilon_g</math></b>	6.75	10.39	11.54	12.95	16.07
	<b>Plane 3 <math>\epsilon_g</math></b>	6.77	9.62	11.91	11.82	13.39
	<b><math>\Delta \epsilon_g</math></b>	0.02	-0.78	0.37	-1.12	-2.67
<b>W31</b>	<b>Plane 2 <math>\epsilon_g</math></b>	8.09	9.61	12.47	13.03	17.41
	<b>Plane 3 <math>\epsilon_g</math></b>	7.10	10.44	13.52	11.79	16.04
	<b><math>\Delta \epsilon_g</math></b>	-0.99	0.83	1.05	-1.24	-1.37

**Table XIII: Plane 2 to Plane 3 Gas Holdup 25 PPM**

PPM	RPM	1540	1540	2070	2600	2600
<b>25</b>	<b>LPM</b>	2.5	4.5	3.5	2.5	4.5
<b>MIBC</b>	<b>Plane 2 <math>\epsilon_g</math></b>	6.74	9.27	10.72	11.64	15.48
	<b>Plane 3 <math>\epsilon_g</math></b>	7.44	10.38	9.82	11.02	17.46
	<b><math>\Delta \epsilon_g</math></b>	0.70	1.11	-0.90	-0.62	1.98
<b>H27C</b>	<b>Plane 2 <math>\epsilon_g</math></b>	6.75	10.39	11.54	12.95	16.07
	<b>Plane 3 <math>\epsilon_g</math></b>	7.64	11.86	11.91	12.86	17.70
	<b><math>\Delta \epsilon_g</math></b>	0.88	1.47	0.37	-0.09	1.63
<b>W31</b>	<b>Plane 2 <math>\epsilon_g</math></b>	8.09	9.61	12.47	13.03	17.41
	<b>Plane 3 <math>\epsilon_g</math></b>	8.02	10.75	13.52	12.84	18.48
	<b><math>\Delta \epsilon_g</math></b>	-0.07	1.14	1.05	-0.20	1.06

#### 4. Gas holdup rate

**Table XIV** displays gas holdup percentage increases for each frother at 5 ppm and 25 ppm. The table calculates the percentage increase between minimum and maximum values achieved for each plane, shown as Min to Max. Plane 1 to Plane 2 compares the increase factor between planes for minimum and maximum values for each frother. Factors for each frother are similar both between minimum and maximum runs and between planes on the same test. Total gas holdup increases in ascending order from MIBC to W31 with the factor increase of gas holdup between the sensor planes ranging from 10 – 20%. The results shown in **Table XIV** suggest a relationship between the rate at which gas holdup builds relative to the height

**Table XIV: Gas holdup increase percentage**

		5 PPM			25 PPM		
		MIBC	H27C	W31	MIBC	H27C	W31
Plane 1 $\varepsilon_g$	Min to Max	227%	237%	241%	249%	278%	240%
Plane 2 $\varepsilon_g$	Min to Max	214%	215%	224%	230%	238%	215%
P1 to P2 $\varepsilon_g$	Min	159%	144%	142%	144%	147%	139%
	Max	149%	131%	132%	132%	126%	125%

of the column. Gas dispersion terms were used to derive an equation that considers the increase in gas holdup within the distance between the sensors.

$$E_g = \frac{\varepsilon_2 - \varepsilon_1}{h} * J_g \left( \frac{\varepsilon_g}{s} \right) \quad (2)$$

Where  $E_g$  is the gas dispersion rate,  $\varepsilon_1$  and  $\varepsilon_2$  are gas holdup values at each sensor plane,  $h$  is the distance between sensor planes and  $J_g$  is the superficial gas velocity.

**Table XV** shows the values for  $E_g$  compiled for the 5 ppm and 25 ppm tests for each frother. Pump speeds and gas flow rates are listed from the design of experiment. Comparing values in the table,  $E_g$  is influenced primarily by air flow rates with smaller changes as pump speed increases.

**Table XV: Gas dispersion rates**

	RPM	LPM	$J_g$ (cm/s)	$E_g$ 5 ppm	$E_g$ 25 ppm
<b>MIBC</b>	1540	2.5	0.809	0.33	0.33
	1540	4.5	1.455	0.87	0.95
	2600	2.5	0.809	0.25	0.23
	2600	4.5	1.455	1.13	1.10
<b>H27C</b>	1540	2.5	0.809	0.32	0.35
	1540	4.5	1.455	0.98	0.95
	2600	2.5	0.809	0.21	0.16
	2600	4.5	1.455	0.97	0.97
<b>W31</b>	1540	2.5	0.809	0.34	0.37
	1540	4.5	1.455	1.07	0.84
	2600	2.5	0.809	0.15	0.18
	2600	4.5	1.455	1.11	1.01

The  $E_g$  values from Table 11 were added to Design Expert to test the results within the model. ANOVA results were significant for all three frothers and chart of the response are shown in **Figure 20**, **Figure 21** and **Figure 22**.

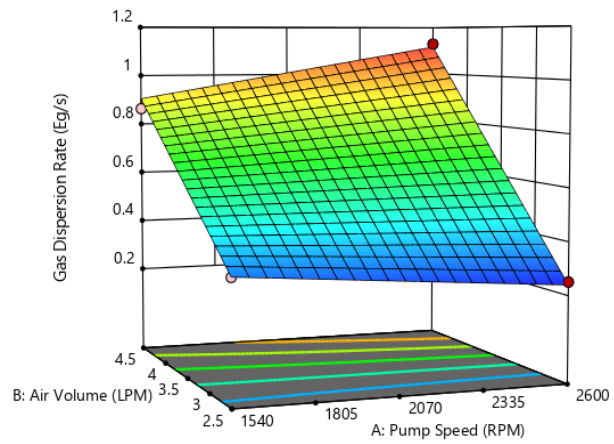


**Figure 20: Eg, MIBC**

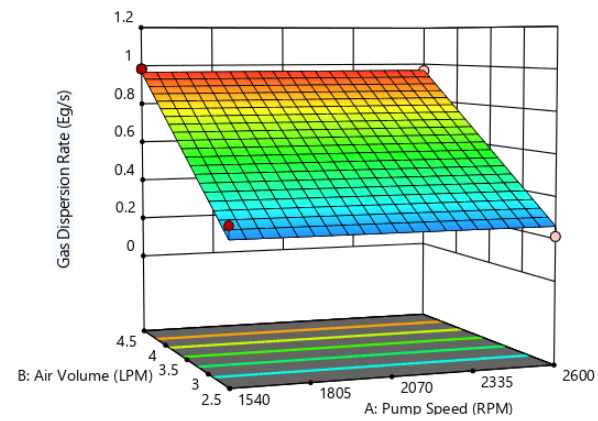
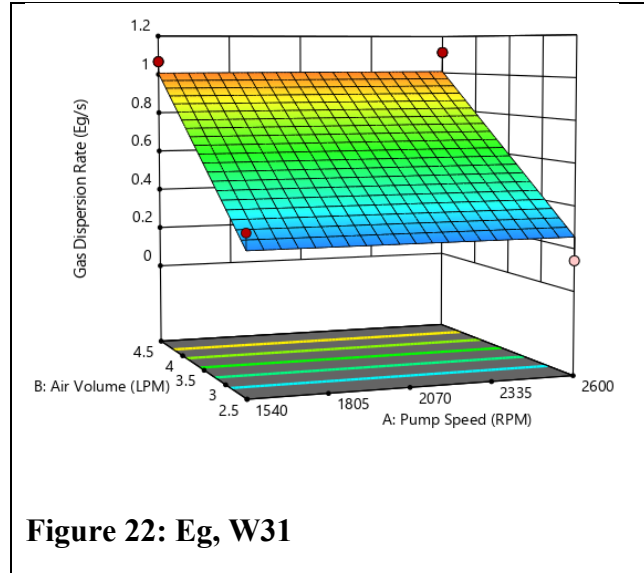


**Figure 21: Eg, H27C**



Comparing **Figure 20** to **Figure 22**, there is no change in  $E_g$  as pump speed increases for both H27C and W31.  $E_g$  increased by  $0.264 \text{ } \epsilon_g/\text{s}$  for MIBC at 4.5 LPM air flows but decreased by  $0.078 \text{ } \epsilon_g/\text{s}$  for 2.5 LPM air flow. High pump speed and low air flow rates gave the lowest  $E_g$ . This is the effect of higher fluid flow rates through the sensing volume. Varying concentration levels had no effect on  $E_g$ . To understand when dispersion is maximized,  $E_g$  was also calculated from plane 2 to plane 3. Referring to **Figure 1**, plane 2 and plane 3 are separated by 40.5 cm. Differences in gas holdup values for plane 3 and plane 4 are statistically insignificant so mean value was used to calculate the values shown in

**Table XVI.** Increases in  $E_g$  over the distance between plane 2 and plane 3 are insignificant compared to the rapid rate seen directly above the sparger.

**Table XVI: Plane 2 to Plane 3 mean gas dispersion rate comparison**

	<b>RPM</b>	<b>LPM</b>	<b>J<sub>g</sub> (cm/s)</b>	<b>E<sub>g</sub> 5 ppm</b>	<b>E<sub>g</sub> 25 ppm</b>	<b>E<sub>g</sub> Mean</b>
<b>MIBC</b>	1540	2.5	0.809	0.33	0.33	0.010
	1540	4.5	1.455	0.87	0.95	0.046
	2600	2.5	0.809	0.25	0.23	0.009
	2600	4.5	1.455	1.13	1.10	0.016
<b>H27C</b>	1540	2.5	0.809	0.32	0.35	0.005
	1540	4.5	1.455	0.98	0.95	0.011
	2600	2.5	0.809	0.21	0.16	0.030
	2600	4.5	1.455	0.97	0.97	-0.024
<b>W31</b>	1540	2.5	0.809	0.34	0.37	0.002
	1540	4.5	1.455	1.07	0.84	0.003
	2600	2.5	0.809	0.15	0.18	0.005
	2600	4.5	1.455	1.11	1.01	0.013



## 5. Three-phase results

### 5.1. Three-phase results and comparisons

To reduce the complexity in the initial three-phase testing the design of experiment only used frother concentration and percent solids as variables. Pump speed was set at 2300 RPM with air flow set at 4.0 LPM ( $J_g = 1.13$  cm/s). Using the same methods as the two-phase testing, the data from the three-phase frother tests was analyzed in Design Expert and compiled in **Table XVII**. Results had a high degree of variance between frothers. MIBC has significant models for

**Table XVII: Three-phase ANOVA results**

			Model	A: Concentration	B: % Solids	Lack of fit
MIBC	Mean	F-value	14.63	14.63		2.73
		p-value	0.0187	0.0187		0.268
	Plane 1	F-value	9.46	9.46		20.89
		p-value	0.0371	0.0371		0.0457
	Plane 2	F-value	16.44	16.44		0.7328
		p-value	0.0154	0.0154		0.5771
Eg	F-value				0.0186	
	p-value				0.9039	
H27C	Mean	F-value	9.54	9.54		1.19
		p-value	0.0366	0.0366		0.4573
	Plane 1	F-value	10.85	10.85		0.8722
		p-value	0.0301	0.0301		0.5341
	Plane 2	F-value	8.3	8.3		1.58
		p-value	0.0449	0.0449		0.3882
Eg	F-value	44.66		42.27	0.0097	
	p-value	0.0001		0.0001	0.9	
W31	Mean	F-value	34.13	43.78	24.48	6.57
		p-value	0.0086	0.007	0.0158	0.1245
	Plane 1	F-value	41.47	53.38	29.56	5.38
		p-value	0.0065	0.0053	0.0122	0.1462
	Plane 2	F-value	27.73	34.8	19.65	6.21
		p-value	0.0119	0.0097	0.0213	0.1304
Eg	F-value					
	p-value					

plane 1 and plane 2 while the mean and  $E_g$  models had F and p-values outside of significant range. All the models created for H27C and W31 were both significant apart from the  $E_g$  model for W31. Comparing H27C and W31 shows that the model for H27C is dependent on frother concentration except for  $E_g$ , which is related to solids content. The solids content is not a significant factor for the gas holdup values for H27C. The model for W31 shows that both frother concentration and solids content affect gas holdup.  $E_g$  for W31 is not significant for any of the variables. Given the highly variable results for the three-phase testing, results for each frother are discussed separately.

### 5.1.1. MIBC Results

**Table XVIII** shows the compiled results of the MIBC tests. The midpoint values (15 ppm, 15 % solids) were averaged from the three tests performed. Reviewing **Table XVII** shows that statistical significance varies by plane. The model for plane 1 is significant but the lack of fit is also significant, meaning that the test results cannot be used to predict outcomes.

**Table XVIII: MIBC Three-phase test results**

Frother	Conc ppm	% Solids	Plane 1 $\epsilon_g$	Plane 2 $\epsilon_g$	Mean $\epsilon_g$	$E_g$	$\Delta \epsilon_g$ P1-P2
MIBC	5	10	8.070	10.420	9.245	0.532	2.350
	5	20	8.851	10.375	9.613	0.345	1.524
	15	15	9.347	11.572	10.460	0.504	2.225
	25	10	12.256	14.820	13.538	0.580	2.564
	25	20	9.993	13.185	11.589	0.723	3.192

Conversely, plane 2 and the mean can be used for prediction.  $E_g$  values only worked for the lack of fit test. Overall, this shows that MIBC results do not create a stable model. Comparing  $E_g$  values in **Table XVIII** shows that there is a factor of 2.1 between the lowest and highest values. Review of the last column of **Table XVIII** shows that at a concentration of 5 ppm and 20 percent

solids, the  $\Delta\epsilon_g$  is 1.524 which indicates that coalescence is a major factor in the low gas holdup increase between plane 1 and plane 2. This agrees with earlier findings that an increase in solids content decreases gas holdup and increases coalescence (Sarhan, et al., 2017). As frother concentration decreases below the critical coalescence concentration, coalescence increases, leading to a decrease in gas holdup (Cho, et al., 2002) . At 25 ppm, above the critical coalescence concentration,  $E_g$  values stabilize and are the same as H27C for both low and high solids concentration and are less than 10% different than W31. Although the MIBC tests did not create a significant model, Design Expert will create charts representing the results that were recorded as shown in **Figure 23**, **Figure 24**, **Figure 25**, and **Figure 26** This serves as a useful visual method to compare the effects relative to the other frothers. The variable with the greatest effect in the initial tests was the frother concentration level. This compares well with the two-phase results where frother concentration has a significant effect on total gas holdup.

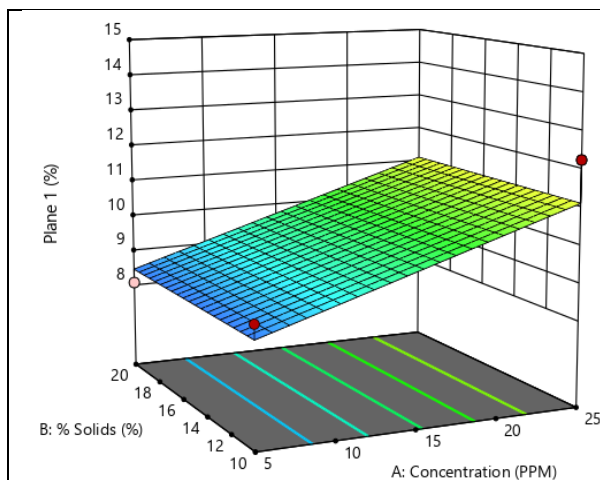


**Figure 23: MIBC plane 1 gas holdup results**

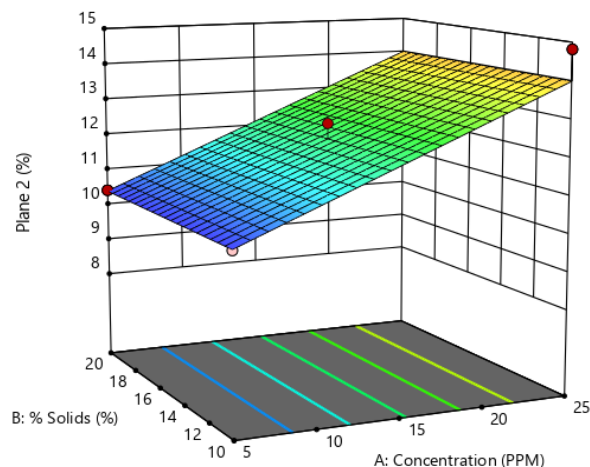


**Figure 24: MIBC plane 2 gas holdup results**

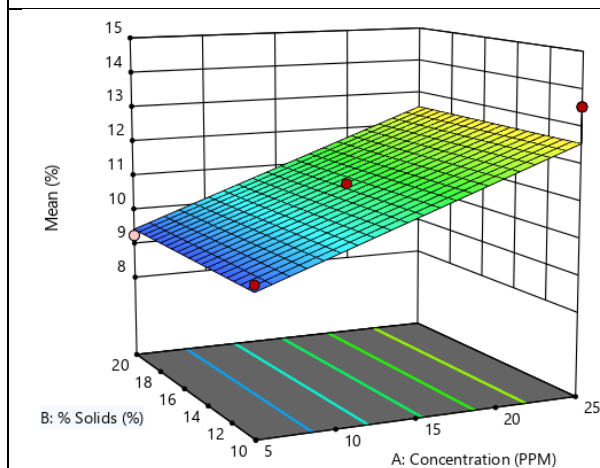


**Figure 25: MIBC mean gas holdup results**

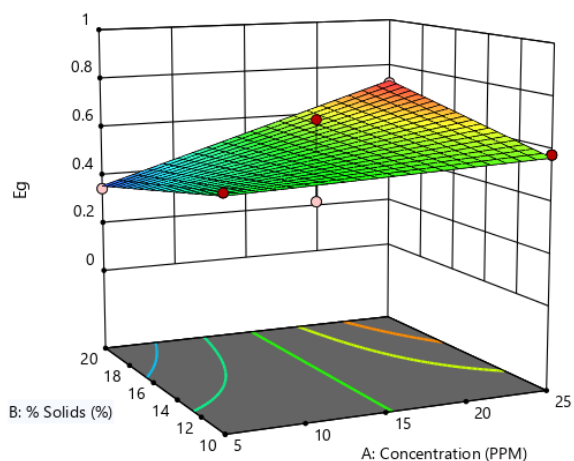


**Figure 26: MIBC  $E_g$  results**

### 5.1.2. H27C Results

The increased strength of H27C creates a more stable system compared to MIBC.

Reviewing **Table XVII** shows that H27C produces significant models for each factor, the only change being the  $E_g$  model which is dependent on percent solids rather than frother concentration. It is hypothesized that with the increase in solids and molecular weight of the frother, bubble momentum decreases and improves dispersion within the column. This effect will

require more testing and research to confirm. Comparing  $E_g$  values in **Table XIX**, there is only a factor of 1.2 between the lowest and highest values. This is attributable to the increased strength of the bubbles in the H27C system which decreases coalescence and stabilizes gas holdup.

Comparing the last column in **Table XVIII** and **Table XIX** ( $\Delta \epsilon_{g P1-P2}$ ) at 5 ppm and 20% solids it can be seen that coalescence leads to lower gas holdup values between plane 1 and plane 2. This demonstrates the importance of frother characteristics in maintaining bubble competence in the pulp zone which is the most turbulent area in the column. The values at 25 ppm are within 0.03 of each other, indicating that frother performance is similar at concentrations above the CCC.

**Table XIX: H27C three-phase test results**

Frother	Conc ppm	% Solids	Plane 1 $\epsilon_g$	Plane 2 $\epsilon_g$	Mean $\epsilon_g$	$E_g$	$\Delta \epsilon_{g P1-P2}$
H27C	5	10	8.746	11.636	10.191	0.654	2.890
	5	20	7.882	10.741	9.312	0.647	2.860
	15	15	8.525	11.779	10.152	0.737	3.255
	25	10	10.396	12.968	11.682	0.582	2.573
	25	20	11.703	14.864	13.284	0.716	3.161

Charts for the H27C tests results are shown **Figure 27**, **Figure 28**, **Figure 29**, and **Figure 30**. Results are like those for MIBC apart from the changes in the  $E_g$  results. As concentration increases at low solids content, gas dispersion decreases. This could be a result of the increased velocity caused by a decrease in the mass of the particle laden bubbles as they move through the two sensor planes. Testing of frothers with higher molecular weights will aid in understanding this effect. This is further reinforced by the sharp increase as the solids loading increases. This is an area that needs further research and additional testing.

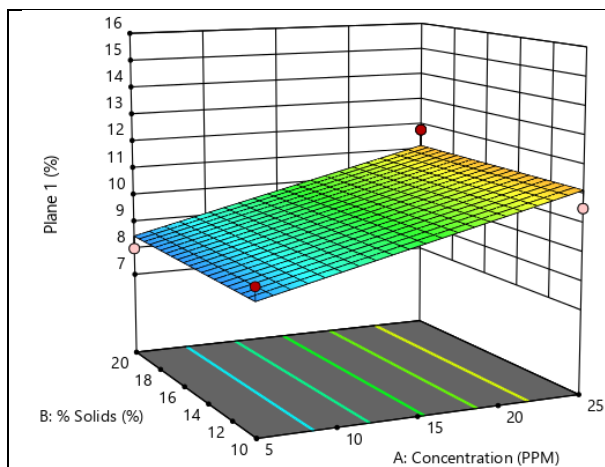


Figure 27: H27C plane 1 gas holdup results

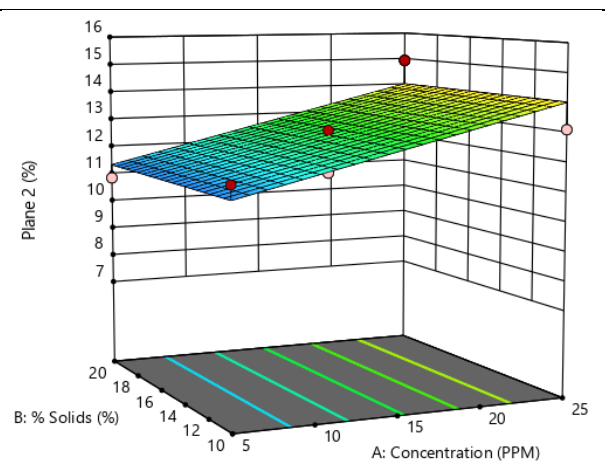


Figure 28: H27C plane 2 gas holdup results

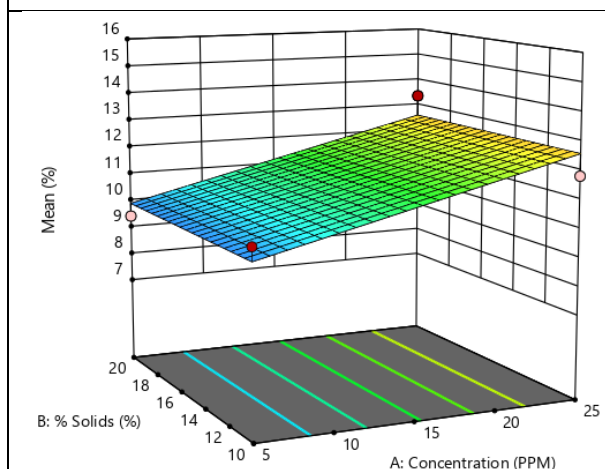


Figure 29: H27C mean gas holdup results

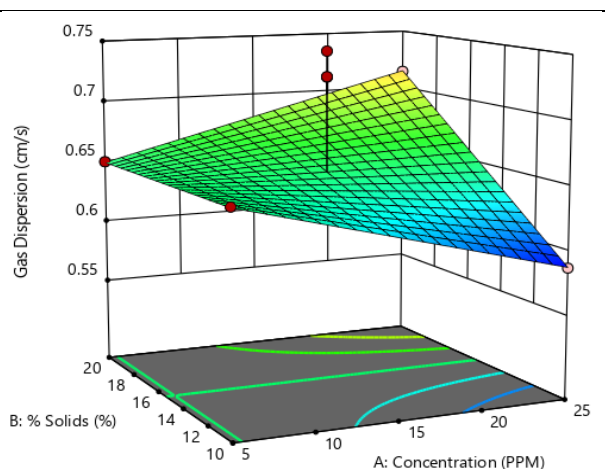


Figure 30: H27C  $E_g$  results

### 5.1.3. W31 Results

W31 gave the most stable results of the three frothers. **Table XX** shows the values for W31. The factor between the lowest and highest values for  $E_g$  is only 1.09 compared to 2.1 and 1.2 for MIBC and H27C, respectively. Similarly, the difference in gas dispersion rate between plane 1 and plane 2 is a maximum of 0.3 %/s, indicating that coalescence is more controlled with a stronger frother. At 5 ppm and 20% solids, the most unstable test for MIBC, W31 maintains

stable gas holdup and gas dispersion values relative to tests at higher concentrations. As with H27C, W31 decreases coalescence in the turbulent pulp zone, stabilizing the bubbles as they move from the collection zone into the froth phase.

**Table XX: W31 three-phase test results**

<b>Frother</b>	<b>Conc ppm</b>	<b>% Solids</b>	<b>Plane 1 <math>\epsilon_g</math></b>	<b>Plane 2 <math>\epsilon_g</math></b>	<b>Mean <math>\epsilon_g</math></b>	<b><math>E_g</math></b>	<b><math>\Delta \epsilon_g</math> P1-P2</b>
W31	5	10	6.690	9.597	8.143	0.658	2.907
	5	20	3.992	6.656	5.324	0.603	2.663
	15	15	7.535	10.094	8.711	0.626	2.558
	25	10	8.963	11.773	10.368	0.636	2.809
	25	20	7.419	10.323	8.871	0.657	2.904

Charts for the W31 results are shown in **Figure 31**, **Figure 32**, **Figure 33**, and **Figure 34**. These figures show the influence of solids content on total gas holdup, reducing total gas holdup as shown in previous research (Banisi, 1995). An interesting observation from comparing charts is that only W31 shows the effect of the increase in solids content. This effect could be the result of the increased stability of the bubbles in the W31 tests, allowing the effect to be captured by the ERT.

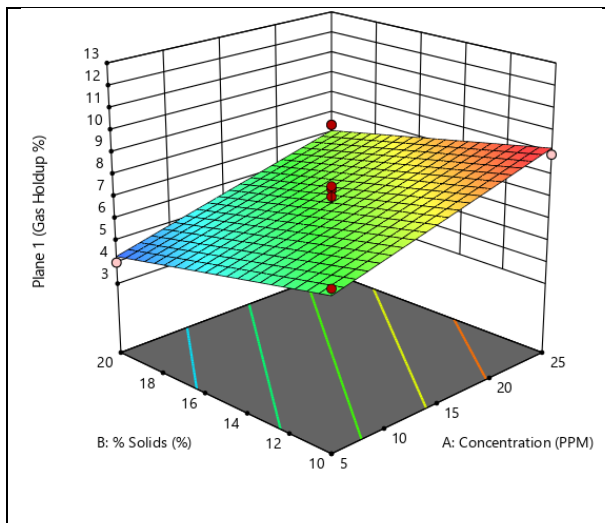


Figure 31: W31 plane 1 gas holdup results

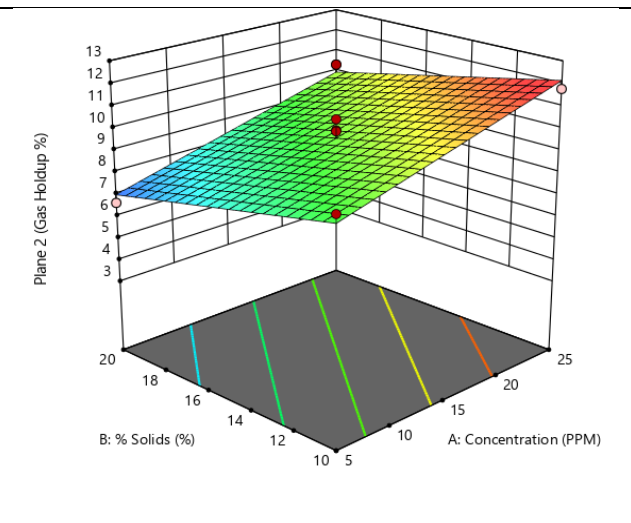


Figure 32: W31 plane 2 gas holdup results

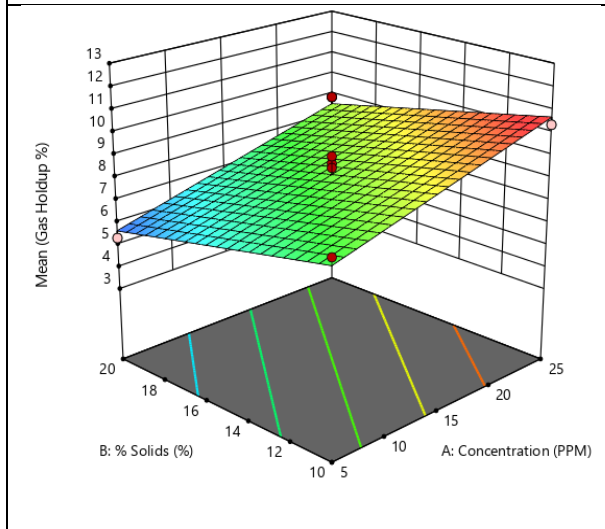


Figure 33: W31 mean gas holdup results

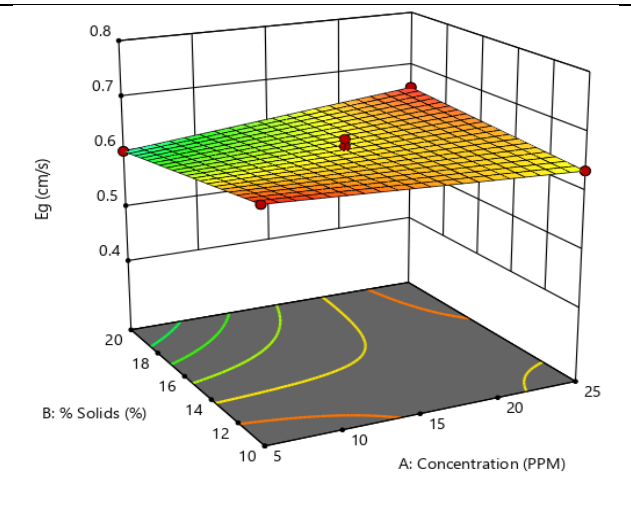


Figure 34: W31 Eg results

### 5.1.4. H27C block test results

Given the variability between frother results, after completing the two factor tests for all three frothers a block test was designed to determine if conditions such as barometric pressure and temperature play a role in test results. Air flow was added as an additional parameter for the block tests to determine the role of air flow on gas holdup in the presence of solids. A total of 14



tests were conducted, seven tests on two separate days. Results were compiled and Design Expert produced the ANOVA results shown in **Table XXI**. Significant results were achieved for the block test with frother concentration and air flow as the significant factors in the tests.

**Table XXI: Block test ANOVA results**

			Model	A: Concentration	B: % Solids	C: Air Volume	Lack of fit
<b>H27C</b>	Mean	F-value	37.51	37.37		34.1	0.1971
		p-value	0.0001	0.0003		0.0004	0.9276
	Plane 1	F-value	38.47	37.74		27.84	0.1947
		p-value	0.0001	0.0003		0.0007	0.929
	Plane 2	F-value	32.66	32.62		35.59	0.2553
		p-value	0.0001	0.0004		0.0003	0.8927
	Eg	F-value	30.03			30.03	0.8405
		p-value	0.0003			0.0003	0.5964

While there were differences between the conditions for each of the tests, the results achieved still produced a significant model. In addition, a confirmation test was performed to verify the results of the block test. The confirmation test was created in Design Expert and the results are shown in **Table XXII**.

**Table XXII: Block test confirmation results**

<b>Confirmation Test</b>							
Concentration	% Solids	Air Volume					
30	15	4.5					
<b>Response Data</b>							
Plane 1	Plane 2	Mean					
9.438	13.122	11.280					
Response	Predicted Mean	Predicted Median	Std Dev	SE Pred	95% PI low	Data Mean	95% PI high
Plane 1*	9.72203	9.72203	0.80278	0.96549	7.496	9.438	11.948
Plane 2*	11.3646	11.3646	1.24875	1.50184	7.901	13.122	14.828
Mean*	6.64715	6.64715	2.10779	2.18176	1.845	11.280	11.449

As shown in **Figure 35** to **Figure 37** gas holdup is a combination of frother concentration and air volume in the block test. Gas dispersion effects are principally reliant on air volume which matches the findings of the two-phase tests as shown in **Figure 20**, **Figure 21** and **Figure 22**.

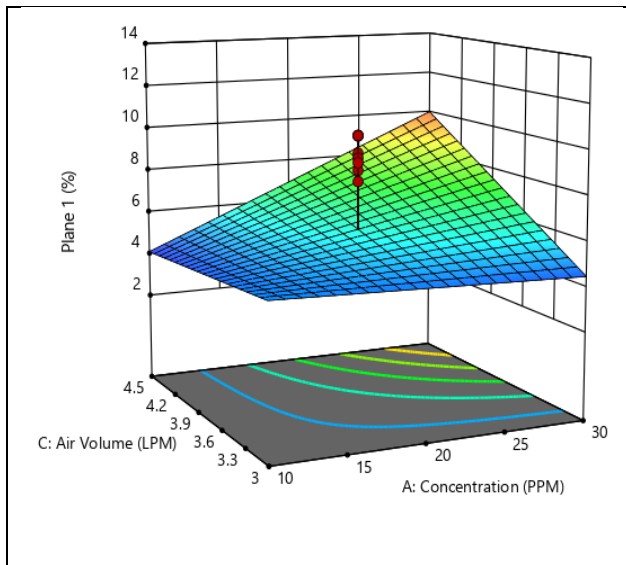


**Figure 35: Plane 1 gas holdup for H27C block test**

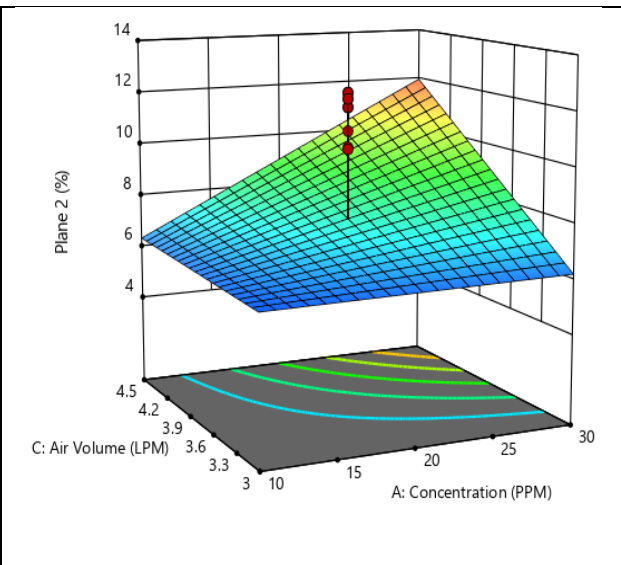


**Figure 36: Plane 2 gas holdup for H27C block test**

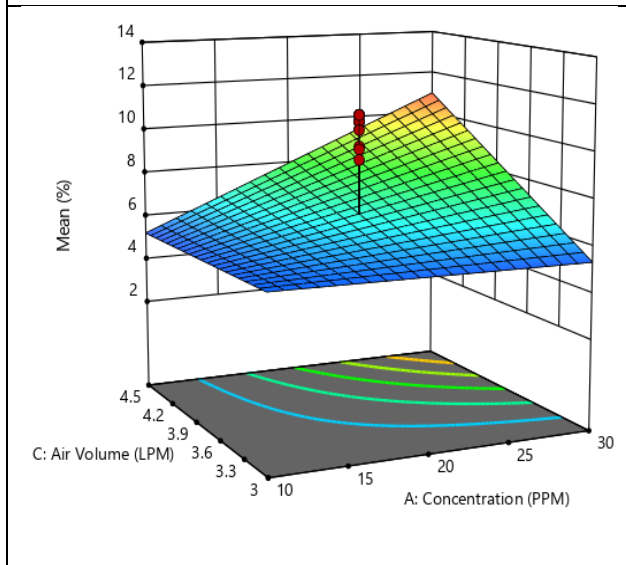


**Figure 37: Mean gas holdup for H27C block test**

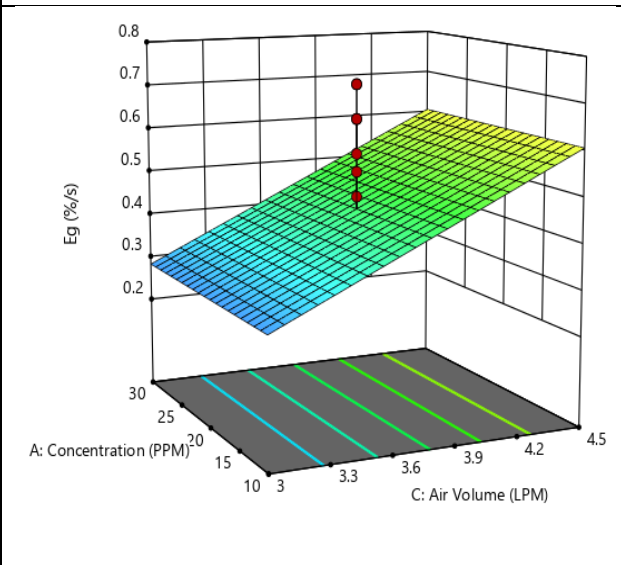


**Figure 38:  $E_g$  for H27C block test**

## 5.2. Three-phase results discussion

The models created by Design Expert are essential in comparing the results of the testing completed for each frother. There are significant differences in the results between the three frothers tested and Design Expert allows for these differences to be analyzed and visualized quickly.

The unique results of the W31 tests in which the gas holdup decreases with the increase in percent solids of the slurry requires further investigation and possibly the testing of even stronger frothers to determine if the results can be repeated. Understanding the possible mechanisms for this effect, in the stronger frothers when compared to weaker frothers, is essential in predicting the behavior of various frothers.

MIBC starts to perform more like the stronger frothers as concentration increases past the CCC. At low concentration MIBC is unstable and results becomes unreliable. Coupled with the poor performance for gas dispersion rate, the MIBC data indicates that there is the possibility of poor solids flotation rates and collection efficiency at the lab scale and possibly at the plant scale. This does not appear to be the case with H27C or W31 which performed more consistently across the range of concentrations tested.

## 6. Conclusions and future work

- ERT is an effective method to determine gas holdup concentrations throughout a flotation column. By positioning the sensor near the sparger it is possible to quantify the behavior of various frothers, frother concentrations and mechanical parameters and their effect on gas holdup.
- Stronger frothers increase gas holdup when frother concentration, pump speed and air flow are increased. This is due to the increased stability imparted to the froth by higher concentrations and stronger frother. The relative increase in gas holdup is similar for all frothers with stronger frothers producing higher overall gas holdup values.
- The gas dispersion rate is correlated to the air flow passing through the sparger. Increased gas added to the system increases the bubble surface area flux, increasing gas holdup. Frother type, concentration and pump speed have little or no effect on the gas dispersion rate. Gas dispersion does not substantially increase after the first few centimeters past the sparger outlet.
- Continued testing of stronger frothers will determine the effect of slurry solids content on gas dispersion and the stability of the axial dispersion rate.
- Future testing will correlate fundamental gas dispersion values and frother strength to total recovery of solids and recovery efficiency.
- Additional ore types need to be investigated, as well as the effect of collector and depressant chemicals, as they relate to total gas holdup in the column.

## References

- Aw, Suzanne Ridzuan, et al. 2014.** Electrical Resistance Tomography: A review of the application of conducting vessel walls. *Powder Technology*. January 2014, pp. 256-264.
- Azgomi, F., Gomez, C.O. and Finch, J.A. 2006.** Characterizing frothers using gas holdup. *The Canadian Journal of Metallurgy and Materials Science*. 2006, pp. 237-242.
- . **2007.** Correspondence of gas holdup and bubble size in presence of different frothers. *International Journal of Mineral Processing*. March 19, 2007, pp. 1-11.
- Banisi, S. and Finch, J.A. 1994.** Reconciliation of bubble size estimation methods using drift flux analysis. *Minerals Engineering*. 1994, pp. 1555-1559.
- Banisi, S., Finch, J.A., Laplante, A.R. 1995.** Effect of solid particles on gas holdup in flotation columns - 1. Measurement. *Chemical Engineering Science*. 1995, pp. 2329-2334.
- Cho, Y.S. and Laskowski, J.S. 2002.** Effect of flotation frothers on bubble size and foam stability. *International Journal of Mineral Processing*. July 2002, pp. 69-80.
- Farrakhpay, Saeed and Bradshaw, Dee. 2012.** Effect of clay minerals on froth stability in mineral flotation: A review. *International Mineral Processing Congress 2012 Proceedings*. September 24-28, 2012.
- Finch, J.A. and Dobby, G.S. 1990.** *Column Flotation*. Oxford : Pergamon Press, 1990.
- G.S., Dobby and Finch, J.A. 1985.** Mixing characteristics of industrial flotation columns. *Chemical Engineering Science*. 1985, pp. 1061-1068.
- Gomez, C.O. and Finch, J.A. 2007.** Gas dispersion measurements in flotation cells. *International Journal of Mineral Processing*. 2007, pp. 51-58.
- . **2002.** Gas dispersion measurements in flotation machines. *CIM Bulletin*. 2002, pp. 73-78.

**Kuan, Seng How and Finch, James A. 2010.** Impact of talc on pulp and froth properties in F150 and 1-pentanol frother systems. *Minerals Engineering*. April 10, 2010, pp. 1003-1009.

**Nesset, J.E., Hernandez-Aguilar, J.R., Acuna, C., Gomez, C.O., Finch, J.A. 2005.** Some gas dispersion characteristics of mechanical flotation machines. *Minerals Engineering*. November 2005, pp. 807-815.

**Nissinen, Antti, et al. 2014.** Estimation of the bubble size and bubble loading in a flotation froth using electrical resistance tomography. *Minerals Engineering*. July 2014, pp. 1-12.

**Ross, V., Singh, A. and Pillay, K. 2019.** Improved flotation of PGM tailings with a high-shear hydrodynamic cavitation device. *Minerals Engineering*. April 2019, pp. 133-139.

**Sarhan, A.R., Naser, J. and Brooks, G. 2017.** Effects of particle size and concentration on bubble coalescence and froth formation in a slurry bubble column. *Particuology*. 2017.

**Singh, Brajesh K., Quiyoom, Abdul and Buwa, Vivek V. 2017.** Dynamics of gas-liquid flow in a cylindrical bubble column: Comparison of electrical resistance tomography and voidage probe measurements. *Chemical Engineering Science*. 2017, pp. 124-139.

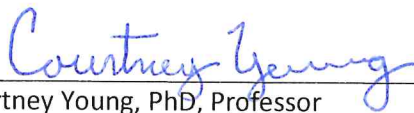
**Wills, B.A. and Finch, J.A. 2016.** *Wills' Mineral Processing Technology, Eighth Ed.* Oxford : Elsevier, 2016.

**Zhou, Z.A., et al. 2009.** On the role of cavitation in particle collection in flotation - A critical review 2. *Minerals Engineering*. January 2009, pp. 419-433.

**Zhou, Z.A., Xu, Zhenghe and Finch, J.A. 1994.** On the role of cavitation in particle collection during flotation - A critical review. *Minerals Engineering*. March 1994, pp. 1073-1084.

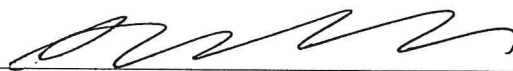
## SIGNATURE PAGE

This is to certify that the thesis prepared by Philip Holdsworth entitled "EFFECT OF FROTHER STRENGTH AND SOLIDS ON GAS DISPERSION IN A CAVITATION SPARGER MEASURED BY ELECTRICAL RESISTANCE TOMOGRAPHY" has been examined and approved for acceptance by the Department of Metallurgical and Materials Engineering, Montana Technological University, on this 15<sup>th</sup> day of April, 2020.



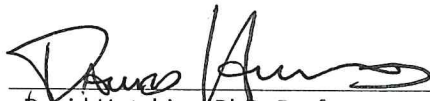
---

Courtney Young, PhD, Professor  
Department of Metallurgical Engineering  
Chair, Examination Committee



---

Richard LaDouceur, PhD, Adjunct Faculty  
Department of Metallurgical Engineering  
Member, Examination Committee



---

David Hutchins, PhD, Professor  
Department of Environmental Engineering  
Member, Examination Committee